Atmos. Chem. Phys. Discuss., 13, 13967–14035, 2013
www.atmos-chem-phys-discuss.net/13/13967/2013/
doi:10.5194/acpd-13-13967-2013

Atmospheric Chemistry and Physics Discussions

Multi-year objective analyses of warm season ground-level ozone and $PM_{2.5}$ over North America using real-time observations and Canadian operational air quality models

A. Robichaud and R. Ménard

Atmospheric Science and Technology Directorate, Environment Canada, 2121 Trans-Canada Highway, Dorval (Québec), H9P1J3, Canada

Received: 28 February 2013 – Accepted: 7 May 2013 – Published: 28 May 2013

Correspondence to: A. Robichaud (alain.robichaud@ec.gc.ca)

Published by Copernicus Publications on behalf of the European Geosciences Union.

Abstract

We present multi-year objective analyses (OA) on a high spatio-temporal resolution (15 or 21 km, every hour) for the warm season period (1 May–31 October) for ground-level ozone (2002–2012) and for fine particulate matter (diameter less than 2.5 microns ($PM_{2.5}$)) (2004–2012). The OA used here combines the Canadian Air Quality forecast suite with US and Canadian surface air quality monitoring sites. The analysis is based on an optimal interpolation with capabilities for adaptive error statistics for ozone and $PM_{2.5}$ and an explicit bias correction scheme for the $PM_{2.5}$ analyses. The estimation of error statistics has been computed using a modified version of the Hollingsworth–Lönnberg's (H–L) method. Various quality controls (gross error check, sudden jump test and background check) have been applied to the observations to remove outliers. An additional quality control is applied to check the consistency of the error statistics estimation model at each observing station and for each hour. The error statistics are further tuned "on the fly" using a χ^2 (chi-square) diagnostic, a procedure which verifies significantly better than without tuning. Successful cross-validation experiments were performed with an OA set-up using 90 % of observations to build the objective analysis and with the remainder left out as an independent set of data for verification purposes. Furthermore, comparisons with other external sources of information (global models and $PM_{2.5}$ satellite surface derived measurements) show reasonable agreement. The multi-year analyses obtained provide relatively high precision with an absolute yearly averaged systematic error of less than 0.6 ppbv (parts per billion by volume) and 0.7 $\mu g\,m^{-3}$ (micrograms per cubic meter) for ozone and $PM_{2.5}$ respectively and a random error generally less than 9 ppbv for ozone and under 12 $\mu g\,m^{-3}$ for $PM_{2.5}$. In this paper, we focus on two applications: (1) presenting long term averages of objective analysis and analysis increments as a form of summer climatology and (2) analyzing long term (decadal) trends and inter-annual fluctuations using OA outputs. Our results show that high percentiles of ozone and $PM_{2.5}$ are both following a decreasing trend overall in North America with the eastern part of United States (US)

ACPD
13, 13967–14035, 2013

presenting the highest decrease likely due to more effective pollution controls. Some locations, however, exhibited an increasing trend in the mean ozone and $PM_{2.5}$ such as the northwestern part of North America (northwest US and Alberta). The low percentiles are generally rising for ozone which may be linked to increasing emissions from emerging countries and the resulting pollution brought by the intercontinental transport. After removing the decadal trend, we demonstrate that the inter-annual fluctuations of the high percentiles are significantly correlated with temperature fluctuations for ozone and precipitation fluctuations for $PM_{2.5}$. We also show that there was a moderately significant correlation between the inter-annual fluctuations of the high percentiles of ozone and $PM_{2.5}$ with economic indices such as the Industrial Dow Jones and/or the US gross domestic product growth rate.

1 Introduction

Long-term series of surface objective analyses of chemical species are valuable products for understanding the historical evolution of pollution, providing long-term comparisons with models, building a climatology of surface pollutants, evaluating the efficiency of existing pollution control and abatement measures and regulations and supporting epidemiological studies. Among the most two important surface pollutants are ground-level ozone and $PM_{2.5}$. These pollutants are the main constituents of smog and, together with NO_2, form the basis of the Canadian Air Quality Health Index (AQHI, Stieb et al., 2008).

Ozone is not directly emitted but produced by complex photochemical reactions of nitrogen oxides (NO_x) and volatile organic compounds (VOCs) from natural and anthropogenic sources. In urban areas, over one hundred chemical reactions could be involved in ozone production (Jacobson, 2002; Seinfeld and Pandis, 2006). It has been known for a long time that ozone is an oxidant which impacts health (Hazucha et al., 1989; Berglund et al., 1991), exacerbates asthma especially with simultaneous presence of allergenic pollen (White et al., 1994; Newman-Taylor, 1995; Cashel et al.,

ACPD
13, 13967–14035, 2013

2004), impacts agricultural productivity (Skärby and Selldén, 1984; Tingey et al., 1991) causes injuries and additional stress to forest ecosystems (Reich, 1987; Chevone and Linzon, 1988; Badot, 1989; Chappelka and Flagler, 1991) damages materials and cracks rubber and polymers (Cass, 1991). Ozone is also an important source of the hydroxyl radical which breaks down many pollutants and certain greenhouse gases (GHG) and acts itself as an effective GHG (Jacobson, 2002; IPCC, 2007; Houghton, 2009). The atmospheric lifetime of tropospheric ozone is of the order of few weeks above the boundary layer (Tarasick et al., 2010) and down to few hours at night near the surface (IPCC, 2007).

$PM_{2.5}$ is another hazardous pollutant. It consists of aerosols of solid matter which can be manmade (mostly by burning of fossil fuels in power plants or vehicles and various industrial processes) or produced naturally (volcanoes, dust storms, forest or grass fires and sea spray). Those solid aerosols can cool or warm the atmosphere via interaction with incoming solar radiation (aerosol direct effect), or via their ability to act as cloud condensation or ice nuclei and thus play a role in cloud formation (indirect effect) (Hobbs, 1993; Jacobson, 2002; IPCC, 2007; Houghton, 2009). Health impacts of $PM_{2.5}$ are also numerous including promoting asthma (Cashel et al., 2004; Newman-Taylor, 1995) and other respiratory problems (ALA, 2012), stimulating high plaque deposits in arteries producing vascular inflammation, oxidative stress and atherosclerosis (a hardening of the arteries which reduces their elasticity) leading to heart attacks and related cardiovascular problems (Pope et al., 2002; Sun et al., 2005; Reeves, 2011). Together, ozone and $PM_{2.5}$ trigger bronchial micro-lesions which facilitate the penetration of macromolecules such as pollen augmenting the allergenic reaction (Gervais, 1994). Table 1 briefly summarizes the main environmental and health issues related with both pollutants. Given the above evidence, it is therefore of paramount importance to provide to the public and health specialists with the best information about these pollutants.

In this paper, we adopt an optimal interpolation (OI) technique to produce a long-term series of ground-level ozone and $PM_{2.5}$ concentrations over a large region at a rela-

ACPD
13, 13967–14035, 2013

tively low cost. The analyses are not used as initial conditions to the model but are obtained off-line. Nevertheless, they are the best combination of model and observations available to reduce analysis errors. Models are generally characterized by known deficiencies whereas measurement systems suffer from representativeness problems and lack of sufficient coverage therefore providing often only local information. OI as used in operational meteorology for decades provides a framework to extract the maximum information of both model and observations in an optimal way (Rutherford, 1972; Daley, 1991; Kalnay, 2003; Brasnett, 2008). Producing maps of objective analysis based on OI on a regular basis has numerous applications in air quality: (1) initializiation of numerical models at regular time interval (usually every 6 or 12 h) with appropriate fields having overall bias and error variance which are ideally minimum (Blond and Vautard, 2004; Tombette et al., 2008; Wu et al., 2008), (2) providing users with a more accurate picture of the *true state* of a given variable by using an appropriate optimal blend of model fields together with observations so that it produces the best possible analysis (given available data) not only in the vicinity of observation points but elsewhere in a given domain even where the observation network has not an optimal density, (3) building potentially useful maps of health indices (Air Quality Health Index), environmental indices or pollutant loadings on ecosystems (see for example Robichaud and Ménard, 2003) (4) producing surface pollutant climatology (see Sect. 3) (5) providing and mapping temporal trends (see Sect. 5).

One of the key ingredients of data assimilation, or objective analysis is error statistics. However, prescription of adequate error statistics for air quality can be challenging. Unlike the free troposphere or the stratosphere, the boundary layer problems and complex topography make difficult to produce error covariance statistics for ground pollutant such as ozone (Tilmes, 1999, 2001). Moreover, models are often imprecise over complex boundary layer surfaces. Fortunately, the relatively flat topography found over eastern and central North America and the importance of transport of ozone and $PM_{2.5}$ above and within the boundary layer makes these pollutants excellent candidates for objective analysis and data assimilation since the correlation length is much larger than

ACPD
13, 13967–14035, 2013

model resolution so that information can be spread around efficiently over more than one model grid point. Production of a long series of multi-year analyses retrospectively may also pose many other technical problems causing discontinuities or inconsistencies in time series, namely, changes of model version, set of emissions inventories out of date or imprecise, changes in instrumentation through the years, etc. Special attention is thus given here to (1) obtaining optimal (adaptive) error statistics which can follow and adapt to changes over time and (2) to the reduction, as much as possible, of systematic errors so that the analyses form an unbiased and consistent and coherent data set throughout the whole period.

Multi-year analyses presented here combine the information provided by a long series of air quality model outputs from the Canadian Air Quality Regional Deterministic Prediction System (AQRDPS), that is CHRONOS (Canadian and Hemispheric Regional Ozone and NO_x System) model for the period 2002–2009 and GEM-MACH (Global Environmental Multi-scale coupled with Model of Air quality and CHemistry) for the period 2010–2012. The observations used during the same period are taken from US and Canadian surface monitoring networks. One of the main applications of OA, which is presented in this paper, is a summer (June-July-August) climatology. Other methods to derive a multi-year climatology within the troposphere exist such as the traditional spatial domain-filling techniques using observations and trajectories (Tarasick et al., 2010). However, uncertainties of 30–40 % are noted with the meteorological inputs of trajectory models (Harris et al., 2005). Moreover, in the boundary layer, complex dispersion and turbulence tends to render trajectories near the surface less precise than that of higher levels as reported by Tarasick et al. (2010). The multi-year analyses as a form of climatology presented here avoids the process of high uncertainties associated with back trajectories near the surface. The spatial interpolation is naturally accomplished through exponential functions (see Sect. 2.1) so that meteorological and chemical patterns from the model are preserved. While numerous works on stratospheric ozone climatology based on satellite observation combined with various mapping techniques appeared in the last decade or so (Fortuin and Kelder, 1998;

ACPD
13, 13967–14035, 2013

McPeters et al., 2007; Ziemke et al., 2011) as well as for tropospheric climatology, the latter being mostly based on ozonesondes (Logan, 1999; Tarasick et al., 2010), comparatively little work has been done concerning multi-year analyses or climatology specifically for ground-level ozone and $PM_{2.5}$ for North America. The MACC (Monitoring Atmospheric Composition and Climate) reanalysis project of the global tropospheric composition (http://www.gmes-atmosphere.eu/about/project/) is one of the few initiatives to produce a long series of surface and tropospheric pollutant analyses but has a focus in Europe. RETRO-40 (REanalysis of the TROpospheric chemical composition over the past 40 yr, http://retro.enes.org) is also a project of global re-analyses initiated in Europe as well. The decadal series of analyses for ground-level ozone and $PM_{2.5}$ presented in our paper are delivered on a comparatively high spatio-temporal resolution (15 km or 21 km – on an hourly basis) and focuses on the surface for North America.

The rest of our manuscript is organized as follows: Sect. 2 describes the methodology and theory of OA and the models and observation systems used. Section 3 presents results of long term averages of OA, the CHRONOS era (2002–2009) and the GEM-MACH era (2010–2012), from which summer climatology is derived for both periods. Section 4 provides cross-validation and external comparison of OA results. Section 5 introduces pollution trends and analyzes inter-annual fluctuations obtained using OA. Section 6 provides a discussion about certain aspects of the methodology and special issues related to OI and finally Sect. 7 contains a summary and conclusions.

2 Methodology

2.1 The analysis scheme

In this study, the analysis scheme adopted is an optimal combination of model concentrations and observations based on an optimum interpolation method specifically

ACPD
13, 13967–14035, 2013

adapted to surface air quality problems. The basics of the analysis scheme is described in Ménard and Robichaud (2005). The basic goal of an analysis scheme, which we also call "objective analysis", is to find an expression that minimizes the error variance of the combined field of model and observation. It can be shown that this optimization problem yields the following form for the analysis matrix $\mathbf{x}_a^n$ (e.g. Daley, 1991; Kalnay, 2003), that is:

$$\mathbf{x}_a^n = \mathbf{x}_f^n + \mathbf{K}(\boldsymbol{y}_o^n - \mathbf{H}\mathbf{x}_f^n) \quad (1)$$

where $\mathbf{x}_f^n$ is the background field obtained from a short-term forecast, **H** is an operator that performs an interpolation from the model grid point space to the observation space (here we use a bilinear interpolation), $\boldsymbol{y}_o^n$ is the vector that contains all the observations at a given time n, and **K** is the Kalman gain matrix to be defined below. The second term on the right hand side of Eq. (1) is called *analysis increments* (Daley, 1991; Kalnay, 2003) and could be view as the correction to the model due to the observations in order to bring the analyses closer to the *true value*. In variational assimilation schemes, the analysis is obtained through a minimization algorithm, and where the explicit solution (Eq. 1) is never used. However, as in Kalman filters (e.g. Daley 1991; Kalnay 2003) and in OI, Eq. (1) and the Kalman gain matrix **K** are both computed explicitly. The basic difference for OI is that error statistics are stationary and prescribed from past experiments (rather than as time-evolving as in a Kalman filter), and that error correlations are given as functions of space (rather than matrices defined on a specific grid) so that there is no need to interpolate the error correlations onto the observation locations. The computation of the Kalman gain does, however, involve the inversion of a matrix. In meteorology, because of the large number of observations, this inversion is calculated in batches in smaller domains using either data selection or a compactly supported covariance function (Daley, 1991; Houtekamer and Mitchell, 1998). In air quality, the number of surface observations at a given time is limited (in North America about 1,200 observations or less per species) and hence the inversion of the matrix

ACPD
13, 13967–14035, 2013

can be computed directly, so our scheme is equivalent to a 2-D-VAR (two-dimensional variational analysis).

The derivation of the analysis (Eq. 1) is based on the assumptions that: (i) the errors are Gaussian distributed or else the estimate Eq. (1) is a BLUE (Best Linear Unbiased Estimate), (ii) the observation errors are uncorrelated with the background errors, (iii) the observations errors are additive Gaussian noise, and (iv) interpolated observations are linearly related to the model state (e.g. the observation operator is linear). Furthermore, for OI the background error correlation is modeled as a function, generally assumed to be isotropic and homogeneous. In Eq. (1), the gain matrix **K** is given as:

$$\mathbf{K} = (\mathbf{HB})^T (\mathbf{H}(\mathbf{HB})^T + \mathbf{R})^{-1} \quad (2)$$

where **B** is the background error covariance matrix defined on the model grid. But in OI, each term in Eq. (2) is computed as a function between pair of points. For example, for a pair of observation sites k_1 and k_2, we can write:

$$\mathbf{H}(\mathbf{HB})^T (k_1, k_2) = \sigma_f(k_1)\sigma_f(k_2) \exp\{-|x(k_1) - x(k_2)|/L_c\} \quad (3)$$

(assuming here that the background error correlation is an homogeneous isotropic first-order auto-regressive model). The error covariance between a given site k_1 and a particular analysis grid point (i, j) is also given explicitly as:

$$(\mathbf{HB})^T (i, j, k_1) = \sigma_f(i, j)\sigma_f(k_1) \exp\{-|x(i, j) - x(k_1)|/L_c\} \quad (4)$$

which represents the background error covariance between a given station k_1 and the nearest model grid point. **B** is the background error covariance matrix itself, **R** the observation error covariance matrix, $x(k_1)$, $x(k_2)$, the position in space of the corresponding stations k_1 and k_2 and $x(i, j)$, the grid point position. Finally, σ_f and L_c represent respectively the background error variance and the correlation length and is assumed to be constant throughout the domain. However, $\sigma_f(k)$ and $\sigma_o(k)$ for all observation locations k are defined locally and obtained with an autocorrelation model fitting

ACPD
13, 13967–14035, 2013

the observation-minus-forecast residuals, a procedure known as the Hollingsworth–Lonnberg (H–L) method (see Sect. 2.3). Unlike meteorology, where the objective analysis or data assimilation cycle of 6 h are most commonly used (Houtekamer and Mitchell, 1998; Gauthier et al., 1999; Brasnett, 2008), in air quality a cycle of one hour is more appropriate (Blond and Vautard, 2004; Tombette et al., 2008; Wu et al., 2008) since there is a strong diurnal variation of surface pollutants and care must be taken to resolve short or intermittent episodes. Therefore, over the entire study period (2002–2012) our analyses have been produced on an hourly basis. We present here only warm season (1 May–31 October) analyses due to unresolved biases issues for the winter season at the moment for $PM_{2.5}$ and due to the fact that ozone is less of an environmental threat in winter in most cases in North America.

To verify the consistency of the error statistics with the innovations ($\mathbf{d} = \mathbf{y}_o^n - \mathbf{H}\mathbf{x}_f^n$) the Chi-square diagnostic in real-time has been used (Ménard, 2000):

$$\frac{\chi^2}{p} = \frac{\mathbf{d}^T \mathbf{S}^{-1} \mathbf{d}}{p} \approx 1 \tag{5}$$

where p is the number of ingested observations, and

$$\mathbf{S} = \mathbf{H}(\mathbf{HB})^T + \mathbf{R} \tag{6}$$

is the innovation matrix, $\mathbf{d}$ is the innovation vector, and $\mathbf{d}^T$ its transpose. In theory, the value of Chi-square divided by the number of observations should be close to unity (Ménard and Chang, 2000). The matrix $\mathbf{S}$ given by Eq. (6) needs to be inverted only one time per analysis for the non-adaptive scheme, and several times until convergence is achieved in the case of the adaptive scheme (see Sect. 2.3). In both cases, the matrix inversion is performed using a Cholesky decomposition (http://en.wikipedia.org/wiki/Cholesky_decomposition). A potential problem with this method may exist when the matrix $\mathbf{S}$ is moderate to large (typically when the dimension is greater than 1500×1500). In this case, the inversion may become inaccurate and alternative methods should be used. In our study, the maximum number of monitoring

ACPD
13, 13967–14035, 2013

sites used for analyses is always inferior to that number (around 1100 for the period 2002–2009 progressively increasing to around 1300 in 2012). Finally, we remark that the analysis error variance σ_a^2 is always smaller than both the background error variance σ_f^2 and the observation error variance σ_o^2 (e.g. Kalnay, 2003 for a derivation), in fact:

$$1/\sigma_a^2 = 1/\sigma_f^2 + 1/\sigma_o^2 \quad (7)$$

According to Eq. (7), mapping historical evolution of pollutants is therefore more appropriate with an objective analysis being more accurate than model and observations each of them taken separately. Note that Eq. (7) is valid for Gaussian distributions only. Following the same theory, the analysis error **A** could also be derived and has the following form (e.g. Kalnay, 2003 for a demonstration):

$$\mathbf{A} = (\mathbf{I} - \mathbf{KH})\mathbf{B} \quad (8)$$

2.2 Bias correction

Bias correction for analysis is a difficult problem and some hypotheses have to be made in order to solve the problem. Two cases are discussed which have a tractable solution. Either the observation systematic errors are small with respect to the systematic model error or vice versa. In the first case, a model bias correction can be developed as seen below, and in the latter case, we can compute an observation bias correction. When both model and observations have significant biases, a bias correction scheme (for both model and observation) can still be developed but provided that statistics of the bias errors are known and have different characteristic length-scales (see Ménard, 2010). In our study, we assume that the observation bias is small compared to the model bias. This means that the bias correction analysis is used as initial condition for a short-term forecast. Our diagnostic model bias correction goes as follows. Suppose the model bias $\hat{\mathbf{e}}$ is known, an unbiased analysis $\hat{\mathbf{x}}$ is obtained by following equation

ACPD
13, 13967–14035, 2013

(i.e. the sequential form, see Eq. (41) in Ménard 2010):

$$\widehat{\mathbf{x}} = \mathbf{x}_f - \widehat{\mathbf{e}} + \mathbf{K}\left(\mathbf{y}_o - \mathbf{H}(\mathbf{x}_f - \widehat{\mathbf{e}})\right) \tag{9}$$

Note that in Eq. (9) the Kalman gain matrix is standard, that is the same as the one used in Eq. (1). Grouping terms in Eq. (9), gives:

$$\widehat{\mathbf{x}} = \mathbf{x}_f + \mathbf{K}(\mathbf{y}_o - \mathbf{H}\mathbf{x}_f) - (\mathbf{I} - \mathbf{K}\mathbf{H})\widehat{\mathbf{e}} \tag{10}$$

The last term on the right hand side of Eq. (10) can be identified as being the analysis bias. As we assume that the observation bias is small, the residuals $\langle O - A\rangle = \langle \mathbf{y}_o - \mathbf{H}\mathbf{x}_a\rangle$ can be used as a source of information of the analysis bias. Since $\langle O - A\rangle$ is only defined at the observation locations, we extend it to the whole model domain surface, as follows:

$$\mathbf{b}^a = \langle \varepsilon^a \rangle = (\mathbf{I} - \mathbf{K}\mathbf{H})\widehat{\mathbf{e}} = \begin{cases} -\langle O - A\rangle_{\text{region}} & \text{inside the region} \\ -\langle O - A\rangle_{\text{region}} \exp(1 - \Delta^2) & \text{outside the region} \end{cases} \tag{11}$$

with $\langle O - A\rangle_{\text{region}}$ is the time and spatial average of O-A over a certain region. The time average is of 1 month minimum, and different regions are considered: eastern Canada, western Canada, eastern US and western US. The O-A itself are evaluated a posteriori using a previous set of objective analysis. Each region are disjoint and have the shape of an ellipse (instead of a rectangular form) to avoid "corner effects". The bias correction is uniform inside a given region with its value equal to the region average. Outside of a region, the bias correction decays as a function of the square distance Δ^2 defined as,

$$\Delta^2 = \frac{x^2}{a^2} + \frac{y^2}{b^2},$$

where a and b are the ellipse semi-axes, x and y the horizontal distance from the center of the ellipse. The value for a is taken as 1200 km and b is 250 km for the

ACPD
13, 13967–14035, 2013

eastern and western Canadian regions and 700 km for the eastern and western US regions respectively. Outside of all the four regions, the bias correction is the sum of the individual distance-decaying region contributions (bottom part of Eq. (11), e.g. when $\Delta > 1$, the grid point is outside the elliptical region). An analysis bias correction scheme is not necessary for ozone but was applied only to $PM_{2.5}$.

2.3 Adaptive error statistics

Attention should be given to the production of error statistics as it can destroy the effective optimality of an assimilation scheme (Daley 1992; Tilmes, 2001; Sandu and Chai, 2011) and especially in the quality control where a valid observation could be rejected (see Robichaud et al., 2010). The best source of information about error statistics are the innovations (Daley, 1991; Blond and Vautard, 2004). The technique used here consists of pairing up different monitoring sites, calculate the covariance of OmP (Observation minus model Prediction) between the paired stations, plot the result as a function of distance, and fit an autoregressive correlation model as a function of distance but excluding the data at the origin. This method was originally adopted in meteorology by Gandin (1963) using a climatology and by Rutherford (1972) utilizing a short-term forecast. This technique was further developed by Hollingsworth and Lönnberg (1986) and became a standard in the design of optimum interpolation. Note that in our case (surface air quality) not all stations could be adjusted with a correlation function due to insufficient data or due to too much noise in the data. In such a case, a regional average of error statistics is provided as a replacement for these particular stations. Here, we adopt this method but with some modifications as explained below. An example of the application of the method for a typical site (here the Goddard Space Flight air quality monitoring station) is shown in Fig. 1: σ_f^2 is the intercept of the fitted first-order autoregressive model, and σ_o^2 is the residual (or nugget) error variance at zero distance. As a result of the fitting, an estimation of the local isotropic correlation length L_{ci}, at site i is also obtained. Since our correlation model does not allow for non-homogeneous background error correlations, a spatially averaged uniform correlation length is used in

ACPD
13, 13967–14035, 2013

the optimum interpolation computer code. However, we found that using an averaged correlation length as the uniform correlation length scale used in optimum interpolation does not provide an optimal analysis system and some tuning of the error statistics is needed. The tuned error covariance parameters go as follows. Let us introduce scaling factors for the background error variance and length scale, α and β respectively, into the Eqs. (3) and (4):

$$\mathbf{H}(\mathbf{HB})^t(k_1,k_2) = \alpha\sigma_f(k_1)\sigma_f(k_2)\exp\{-|x(k_1)-x(k_2)|/\beta L_c\} \quad (12)$$

for a pair of stations k_1, k_2, and

$$\mathbf{H}(\mathbf{HB})^t(i,j,k_1) = \alpha\sigma_f(i,j)\sigma_f(k_1)\exp\{-|x(i,j)-x(k_1)|/\beta L_c\} \quad (13)$$

for the covariance between a given station k_1 and a model grid point (i, j). The tunable parameters, α and β are then estimated "on the fly" using a re-calculation of the **K** matrix as follows. A sensitivity analysis of the parameters α and β revealed that a lower analysis error can be obtained while approaching a χ^2/p value to one, and thus an adaptive scheme has been developed by using the Chi-square diagnostic "on the fly" to scale the error statistics on an hourly basis. Here is how the algorithm works:

1. Let n be the (first) iterate which we recalculate the Kalman gain (at a given time step). First we iterate on L_c,

$$L_c^{n+1} = \frac{L_c^n}{\left(\frac{\chi_n^2}{p}\right)} \quad (14)$$

until there is convergence or until

$$\frac{\chi^2}{p} \approx 1 \quad (15)$$

The convergent value of L_c that is associated with a Chi-square equal to one is the correlation length scale used in the optimum interpolation code.

ACPD
13, 13967–14035, 2013

2. If needed only if χ^2/p does not reach the value one, then an adjustment on σ_B^2 is performed as well

$$\left(\sigma_B^2\right)^{m+1} = \left(\sigma_B^2\right)^m \left(\frac{\chi_m^2}{p}\right) \tag{16}$$

until the chi-square condition Eq. (15) is reached. We note here that multiple solutions of L_c and σ_B^2 can give the same chi-square, so that the above procedure turns out to be a practical solution to get a better analysis. However, the authors do not claim this method as being a general solution. Nevertheless, it turns out that the major physical effect of the adaptive procedure is to reduce the correlation length and the overall impact is that the systematic error and, to a lesser extent, the random error of the analyses are both reduced significantly (see Sect. 4 for details). The mean value of the correlation length obtained by using the adaptive scheme is reduced to a range between 30–100 km (as opposed to the 75–300 km range obtained from the H–L method, e.g. non-adaptive scheme). This reduced value for the correlation length turns out to be in agreement with the correlation length used in the CMAQ (Community Multiscale Air Quality Modeling System) data assimilation algorithm (e.g. correlation length of 60 km, see Sandu and Chai, 2011). Note that in the free troposphere, the correlation length is about one order of magnitude higher (500–1000 km) according to the literature (Liu et al., 1999; Tarasick et al., 2010; van der A et al., 2010 and others) being more closer to the original H–L results (e.g. not using the adaptive scheme). In order to explain the difference, we suggest that the impact of the boundary layer and the topography is to lower the correlation length. The adaptive scheme requires inverting Eq. (6) several times until convergence. This procedure avoids tedious work of constructing new error statistics set for each hour, season and year as it would be required otherwise in an off-line context (not using the adaptive scheme). Nevertheless, a set of basic errors statistics were constructed for one month during summer for both 2004 (CHRONOS era) and 2012 (GEM-MACH era) while for other periods, the adaptive scheme would

ACPD
13, 13967–14035, 2013

be relied on to adjust for changing conditions. Usually within less than 10 iterations is required to achieve the minimization procedure (satisfying the criteria of convergence within less than 1 %). We use the above methodology to produce a long series of multi-year analyses. Since several million hourly analyses were required for this study, care was taken to limit the CPU time. However, the solver of the Optimal Interpolation scheme was computationally optimized so that an hourly map of objective analysis could be produced within a minute in a typical Linux station with the adaptive scheme (which requires 5 to 10 times more of CPU resources compared to the non-adaptive scheme because of the process of convergence involved).

2.4 Models (trial fields)

In this study, CHRONOS (Canadian Hemispheric and Regional Ozone and NO_x System), a chemical transport model (CTM) used for air quality prediction of oxidants on both regional and hemispheric scale in Canada for almost one decade (Pudykiewicz et al., 1997) has been adopted as the trial field for the first period (2002–2009). Archived operational model outputs have been used and the algorithm of OI applied in an off-line fashion for every hour during the period. CTMs or any air quality models solve the mass balance equation for chemical species (Pudykiewicz et al., 1997). The model has a photochemical module which is the only tool available to provide at every point of a domain chemical transformation and capable to reproduce in an approximate way the chemistry of lower troposphere pollutants (Jacobson, 2002; Pudykiewicz et al., 1997; Seinfeld and Pandis, 2006; Pagowski et al., 2010). For the remaining period (2010–2012), an on-line model GEM-MACH has replaced CHRONOS as the main model of the AQRDPS (Air Quality Regional Deterministic Prognostic System) suite at the Canadian Meteorological Centre (CMC). The domain of both models covers all of North America and the model resolution is 21 km for CHRONOS and 15 km for GEM-MACH. Further details about CHRONOS are available in Pudykiewicz et al. (1997). This CTM was driven by meteorological outputs from the Canadian GEM (Global Environmental Multiscale) model. The reader is referred to Côté et al. (1998) for further

ACPD
13, 13967–14035, 2013

information for the meteorological model GEM. GEM-MACH is a limited area air quality model with the same gas-phase chemistry as CHRONOS but on-line with the meteorological model. Its boundary conditions are driven by the operational version of the regional GEM model (Moran et al., 2012). This new operational model is technically an improvement over CHRONOS model since it uses the same transport scheme as the GEM meteorological model and brings the possibility of full coupling air quality and meteorology in the future.

2.5 Observation system

Figure 2a shows the location of surface observations for ozone used by the OA scheme (valid as summer 2010). The density of sites is high over the eastern US, the West Coast and the Gulf States becoming lower elsewhere in the US and Southern Canada and almost vanishing in Northern Canada and Alaska. For the $PM_{2.5}$ network (Fig. 2b), the number of sites is about two times less although the geographical distribution of sites is fairly similar to that of ozone. Table 2 gives more details about the average number of data available in Canada and US during the warm season for the year 2005 (CHRONOS era) and 2012 (GEM-MACH era). Canadian data includes the Canadian Air and Precipitation Monitoring Network (CAPMon) http://www.ec.gc.ca/natchem, and the Canadian National Air Pollution Surveillance Network (NAPS), http://www.etc-cte.ec.gc.ca. US observations used are all originating from a data repository centralized by Sonoma Tech (official mandatory for US/EPA that is Environmental Protection Agency in United States) in the context of the AIRNow (Aerometric Information Retrieval Now) program (http://www.airnow.gov). Raw data is provided by numerous US local air quality agencies (between 150 and 200 agencies in US) as well as Canadian agencies[1]. AIRNow US/EPA ozone and $PM_{2.5}$ real-time

[1]In Canada, air quality monitoring falls under a provincial jurisdiction and managed by Environment Canada as a partnership (such as in the case of Montreal, MUC - Montreal Urban Community and Metro Vancouver).

ACPD
13, 13967–14035, 2013

data base has been made available to us since 2002 for surface ozone observations for a large part of North America and since 2003 for $PM_{2.5}$. However, we decided to start the multi-year analysis retrospective in 2004 for $PM_{2.5}$ when the observation network became more stable. By 2012, data from around 1300 sites are then provided on an hourly basis from AIRNow plus an extra 100 stations originating from Canadian provinces and territories which are not part of the AIRNow program.

Ozone is usually measured by ultraviolet absorption with instrument requirements specified under the US National Ambient Air quality Standards (NAAQS) (see www.epa.gov/air/criteria.html). Instrument noise error is assumed to be 1 ppbv (one part per billion in volume). However, the standard deviation of the observation error including the representativeness error is believed to be higher than 5 ppbv (Fleming et al., 2003). For $PM_{2.5}$, TEOM (Tapered Element Oscillating Microbalance) has been accepted under NAAQS since 1990 (www.epa.gov/particles/actions.html). Uncertainties due to $PM_{2.5}$ instrument noise are evaluated to $2\,\mu g\,m^{-3}$ (Pagowski et al., 2010). One of the most commonly used $PM_{2.5}$ monitor (TEOM-SES), however, largely underestimate concentrations in winter. The correction needed to account for that depends mostly on temperature especially when the daily temperature is below 10 °C and is due to the volatilization of the particulate mass namely the semi-volatile part (Allen et al., 1997). In our study, we focus on warm season (1 May–31 October) analyses which rarely suffer from this instrument bias problem since temperature is normally above 10 °C during the warm season in US and Southern Canada. How well monitors represent the pollution concentration in a given area depends largely on local sources and sinks, topography and meteorology, monitor location and the spatio-temporal variability (Brauer et al., 2010). Problems about spatial representativeness and other specials issues will be addressed in Sect. 6.

ACPD
13, 13967–14035, 2013

3 Objective analyses and analysis increments for surface ozone and $PM_{2.5}$ over North America

3.1 A climatology of summer pollution

One of the main applications of multi-year series of analyses is to produce a climatology of surface pollutants. Here we build a climatology (ground-level ozone and $PM_{2.5}$) by averaging objective analyses produced using the methodology described in Sect. 2 during the summer months (June-July-August) for all available years in our study. Mapping a climatology with OA is more convenient and more precise than either models or observations (according to Eq. 7) as long as the OA biases are relatively small throughout the whole study period. Figure 3 shows the monitoring of OA systematic (bias) and random (standard deviation) errors for the period 2002–2012 and makes the comparison with the model in use at the time (either CHRONOS or GEM-MACH, see bottom of the figure) for (a) ozone and (b) $PM_{2.5}$. Throughout the study period, the OA systematic error (bias) is near zero for both ozone and $PM_{2.5}$ which is not the case with the model systematic error which is much higher than that of OA and can even change sign due to changes of model version, improvement, change of biogenic and anthropogenic emissions, etc. Note that the random error for OA is approximately two times less than that for model ozone (Fig. 3a) and approximately 1.5 times less for OA-$PM_{2.5}$ as compared to the model (Fig. 3b). Moreover, in Sect. 4, we will show that the very low bias of OA is mostly due to the impact of the adaptive scheme plus the explicit bias correction in the case of $PM_{2.5}$. The fact that OA for ozone and $PM_{2.5}$ are virtually unbiased permits us to use it with confidence for different applications. Figure 4a and b shows average OA outputs for the two main eras (prior to and including 2009 using CHRONOS model and after 2009 using GEM-MACH model). The top panels of both figures are computed averages of all the objective analyses for all hours during the summer (June-July-August) for all available years respectively for ozone (2002–2012) and for $PM_{2.5}$ (2004–2012). The bottom panels are for time valid at 18:00 UTC only (which is approximately midday). The left panels are for ozone and the right panels for $PM_{2.5}$. One can observe

ACPD
13, 13967–14035, 2013

that the highest levels of smog (ozone and $PM_{2.5}$) in both period (CHRONOS and GEM-MACH era) tend to be observed in eastern US (south of the Great lakes) and southern California as expected (according to US/EPA; www.epa.gov, those regions also correspond to the highest frequency of NAAQS non-attainment). Note that the diurnal variation is stronger for ozone than that for $PM_{2.5}$ since the maps at 18:00 UTC (bottom panels) are quite different than the average computed for all hours (top panels). This particular time of the day (e.g. 18:00 UTC) is of interest since (1) during the warm season, the planetary boundary layer is often well mixed so that the pollutant values are more representative of the whole boundary layer rather than just the surface values and (2) 18:00 UTC is roughly coincident with geo-synchronous satellite passage. The analyses of the second era (2010–2012), made up with the GEM-MACH model (Fig. 4b) roughly indicate the same situation as for the CHRONOS era (Fig. 4a) except for an increase of average values of background ozone especially in Northern Canada. Together both Fig. 4a and b (multi-year averaged Objective analyses) represent well a summer climatology for the past decade for ground-level ozone and $PM_{2.5}$ over North America during two model's era at CMC. To our best knowledge, this is the first peer-review manuscript of ground-level climatology (Ozone and $PM_{2.5}$) for North America based on a decade of observations on such a high spatio-temporal resolution. We will examine trends in Sect. 5 for ozone and $PM_{2.5}$ computed from the multi-year analyses.

3.2 Long term averages of analysis increments

In principle, a long term average of analysis increment (correction to the model due to observations, e.g. second term on the right hand side of Eq. (1) reveals among other things how much the model is different from the analysis for various time of the day and for various regions and chemical species. Here, it also permits to analyze and monitor the change of behavior from the CHRONOS era to the GEM-MACH era. Figure 5a and b depict the average analysis increment (AI) for both era (CHRONOS and GEM-MACH respectively). A dipolar structure in the zonal direction of the AI (indicated by + and – on the figure) is noted for ozone during the CHRONOS era (2002–2009) meaning that

ACPD
13, 13967–14035, 2013

the model had the tendency to overestimate in the eastern part of North America and underestimate in the Western part (Fig. 5a, left panels). This behavior is also present for the GEM-MACH model (Fig. 5b, left panels) but negative increments seems to be augmented in the East while positive increments have diminished in the West so that the zonal gradient remains almost unchanged. $PM_{2.5}$ analysis increments climatology reveals that CHRONOS model generally underestimated $PM_{2.5}$ (positive AI, Fig. 5a, right panels) whereas GEM-MACH model overestimated (negative AI) in the eastern US and underestimated (positive AI) in the West leading to the presence of a noticeable zonal dipolar pattern appearing for $PM_{2.5}$ during the GEM-MACH era (Fig. 5b, right panels). Finally, the east-west gradient of analysis increments for $PM_{2.5}$ is stronger in the GEM-MACH model than the CHRONOS model. Observations of persistent AI may give deep insight about the AQ forecasting suite behavior and possible model weaknesses. In principle, patterns in analysis increments or a presence of a dipole (here persistent negative values in eastern US and positive in western US) may reveal structures of compensating model errors. Therefore, a climatology of analysis increment is also essential in monitoring of forecasting systems since it reveals how much is the correction needed to get close to the *true value*. As a fact, the random error has augmented for $PM_{2.5}$ when the switch from CHRONOS to GEM-MACH took place in November 2009 (see Fig. 3b) which is consistent with the above finding about analysis increments patterns. Despite models larger systematic and random errors, fortunately, the OA adaptive scheme naturally dampens erratic model behavior as revealed in Fig. 3. More specifically, it shows a low and steady bias near zero through time.

4 Validation of results

In the previous section, monitoring of model and OA for bias and random error has been presented. However, independent observation validation is required as well. In here, cross validation has been performed which consists of reprocessing the objective analysis but with 90 % of the data to produce OA outputs and leave out 10 % of the

ACPD
13, 13967–14035, 2013

data to perform the verification itself. This group of 10 % of observations have never been seen by the analysis and is hence considered as a set of independent data. Three sets of additional similar verifying experiments are then performed and put together for the final verification. Useful objective analyses should be unbiased, have low random error and high reliability. Three metrics are proposed below to evaluate the performance of the multi-year objective analyses (OA) produced and these metrics are also compared with the model performance. The three metrics for performance evaluation used in the cross-validation are the following: (1) average O-P and O- A (O: observation, P: prediction, A: analysis), (2) standard deviation of O-P and O-A and (3) frequency of being correct within a factor two (FC2) for model and analysis. These metrics together constitute a non-redundant set of metrics (Hanna and Chang, 2004) and were used throughout this study. In fact, the first metric respectively measures the systematic bias, the second, the random error and the third, the reliability. The latter is a more robust measure of the performance which is not sensitive to "outliers" nor "compensating errors" (Hanna and Chang, 2004). In the second part of this section, comparison with other sources of information is exposed (other models for ozone forecasting or satellite climatology for $PM_{2.5}$). In the following subsections, we present in more details the results of independent validation.

4.1 Cross validation tests

Since performing cross validation involves reprocessing of objective analysis several times to obtain sufficient amount of data for verification purposes, only specific years were selected for this. The warm seasons of 2005 and 2007 have been chosen during the CHRONOS era for the validation process for respectively ozone and $PM_{2.5}$ and the year 2011 for both ozone and $PM_{2.5}$ during the GEM-MACH era. These three years cover a wide range of different meteorological situation (see http://www.ncdc.noaa.gov) and provide enough cases so that we are able to conclude with a high degree of statistical confidence (e.g. p value < 0.05) the results obtained herein. The results of the verification for 4 different regions for ozone is shown in Fig. 6. The top left panel is for

ACPD
13, 13967–14035, 2013

all North America during the warm season (1 May–31 October), top right panel is for all Canada, and bottom left and right for eastern USA and western USA respectively. The orange and blue navy curves are in all cases associated respectively with the systematic and random errors for the basic (non-adaptive) objective analyses scheme and the green and cyan curves for the tuned (adaptive scheme) objective analyses. The red curves depict the model systematic errors and the black curves, the model random errors. The latter curves are shown for purpose of reference comparison with OA. A clear reduction of both errors (systematic and random) with the objective analyses at almost any time of the day as compared to the model forecast is obtained. For ozone, the adaptive scheme (tuned error statistics "on the fly") shows the smallest errors (random and systematic: e.g. green and cyan curves) in any regions. Whenever a green dot appears on top (Fisher's test for the variance) and/or bottom (T test for average) for a specific hour, it means that the adaptive versus non-adaptive are significantly different at the level of confidence exceeding 95 % (p value < 0.05).

The performance of the analyses during the warm season of 2007 for $PM_{2.5}$ also in the cross-validation mode is shown in Fig. 7. In this particular verification, a new experiment is introduced that is adaptive (tuned) OA *with bias correction* since it was established that an attempt to explicitly correct the bias for $PM_{2.5}$ was achievable and successful using Eq. (11). For the CHRONOS era it is clearly demonstrated that the adaptive scheme with bias correction (gray and pink curves for systematic and random error respectively) yield the best results overall especially during the daytime period (i.e, more obvious for the 15Z-24Z period, see top and bottom left panels). Finally, Fig. 8 shows that for 2011 (GEM-MACH era), independent verification is also excellent for OA (green and cyan curves respectively) as compared to the model (red and black curves), the latter revealing relatively large biases (also consistent with Fig. 3). Note that in both eras, the verification shows nearly unbiased analyses as compared to the model and much lower random errors as well. Values of FC2 for both Canada and US for both ozone and $PM_{2.5}$ for different hours of the day (00:00 UTC, 06:00 UTC, 12:00 UTC and 18:00 UTC) were also computed (Table 3 and 4). In principle, FC2 values can vary

ACPD
13, 13967–14035, 2013

between 0 (absolutely unreliable) up to 1 (absolutely reliable). It is shown that, overall, the best FC2 scores are obtained with the OA adaptive scheme for ozone and the OA adaptive with bias correction (BC) in the case of $PM_{2.5}$. At any time and anywhere, FC2 scores for OA is largely superior (e.g. more reliable) to that of the model as it should be expected from Eqs. (7) and (8).

4.2 Comparison with other sources (global models and satellite)

In order to complete the validation it is also interesting to compare results with external and totally independent information from various sources available such as model and satellite climatologies. Figure 9 presents objective analyses averaged during the whole year of 2005 (bottom left panel) with comparable yearly outputs from MOZART model (Horowitz et al., 2003; Model for OZone And Related Tracer – version 2: horizontal resolution of 2.8°: upper right panel) and GEM-AQ (Global Environmental Multiscale coupled with Air Quality) model (Kaminski et al., 2008, resolution of 1.5°: bottom right panel). Although the global MOZART (Model for Ozone and Related Tracers) and GEM-AQ models have lower horizontal resolution (few hundreds kilometers) than that of the Canadian AQ model suite (resolution of 21 kilometers for OA-CHRONOS), the comparison is nonetheless instructive. In fact, the general pattern of the two global models is roughly in agreement with the objective analysis (OA) especially near coastlines and the Gulf of Mexico where the uncertainty of OA is higher due to less observations available (see Sect. 6). On the other hand, MOZART overestimates mostly over Northern and Central US compared to OA while GEM-AQ seems to be halfway between MOZART and CHRONOS (GEM-AQ underestimates over most of the US). Note that the CHRONOS model (upper left panel), clearly underestimates ozone over many regions. Interestingly enough, it turns out that the average of the three models (figure not shown) provides a much better agreement with OA than any of each model taken individually. Thus OA could serve as a point of comparison and verification for global or regional models or with global surface climatology such as provided for example by RETRO-4 or MACC.

ACPD
13, 13967–14035, 2013

Figure 10 compares a surface global climatology obtained from the satellite instrument MODIS (Moderate-resolution Imaging Spectroradiometer) for $PM_{2.5}$ for the period 2001–2006 (van Donkelaar et al., 2010) with a climatology obtained from OA for the period 2004–2009 (near 18:00 UTC which is roughly the time of satellite overpass). For the purpose of comparison, the same methodology described as for the warm season was extended to the whole year (both warm and cold season) for the period 2004–2009. Although the years are different, the comparison is again instructive and could indicate flaws or weaknesses in both monitoring systems (OA or satellite). The result of the comparison is that although both climatologies roughly agree, important differences appear over some areas such as Rocky Mountains (Southwest US) and Northern Mexico. These differences could be caused by satellite retrieval artefacts over higher elevation (Randall Martin, personal discussion, January 2012) or by imprecise Mexican emissions not taken care of correctly in the CHRONOS model or due to meteorological conditions (because slightly different period used in the comparison). Other satellite climatology exist for $PM_{2.5}$ such as produced by van Donkelaar et al. (2006) for the period January 2001 to October 2002 and was found similar to that of Fig. 10.

5 A study of decadal trend of warm season pollution

One other important application of a long series of analyses is to calculate temporal trends over different areas in order to evaluate the effectiveness of pollution control measures and regulation. Since multi-year analyses presented here offer low biases and random error (Fig. 3 and Sect. 4), we thus believe it is safe to use them to evaluate trends. Moreover, mapping tendencies and trends using OA is more advantageous than using specific observation sites because: (1) according to Eq. (7), for Gaussian distributions, the overall objective analysis error variance (σ_a^2) is always smaller than the observation variance error (σ_o^2) or the model/background error variance (σ_b^2), (2) OA has a series of quality controls so that outliers have been filtered out more efficiently. Particularly, the background check provides a powerful quality control test which rejects

ACPD
13, 13967–14035, 2013

data which are approximately five times the standard deviation of O-P. For example, the background check is critical to eliminate the zero-span test of the ozone analyzer which sometimes is not filtered out from Canadian observation raw data or to disregard data influenced too heavily by the proximity of local strong sources of $PM_{2.5}$ (e.g. local fires or fireworks), (3) if an observation is missing there is no hole in the spatio-temporal sequence since the background provides a likely value at a specific site whereas it would otherwise cause a break in the observation sequence. Moreover, (4) OA provides maps and permits the study of trends across geographical regions for the whole North America at ounce not only at a single site at the time.

5.1 Mapping summer trends of ozone and $PM_{2.5}$ using OA

5.1.1 Ozone

Maps depicting summer averages (June-July-August) for 2005 (Fig. 11a) and for 2012 (Fig. 11b) have been produced using the OA adaptive scheme scenario described in Sect. 2. The trend in characterizing summer smog is established by the difference of averaged OA between 2012 versus 2005 for ozone. The result is presented in Fig. 11c. The details for each region (in % change for different percentiles, average and standard deviation trends) are given numerically and computed in the observation space in Table 5a. Note that these two years (2005 and 2012) were selected because they both show roughly similar weather regimes over many parts of North America (e.g. temperatures over US were well above long term averages in both years, http://www.ncdc.noaa.gov/temp-and-precip/time-series/). This combination of years is desirable in order to minimize biases caused by meteorological inter-annual fluctuations. Note that the high values of differences near the coastline of Northern America, and over continental Northern Canada are considered as artifacts (unreliable zones in Fig. 11c) and therefore not included in computations in Table 5. The reasons are: (i) very few observations are available in those locations, (ii) a problem with boundary conditions was present with CHRONOS model so that the objective analysis could not

ACPD
13, 13967–14035, 2013

correct the model due to lack of available observations in northeastern Canada and over oceans. Therefore, in these regions where the analysis error is equal to that of the model, the analysis has no skill. In Sect. 6 we will discuss that issue more in details (see Fig. 14a, b). Nevertheless, the results within continental US and southern Canada are believed to be reasonably accurate as demonstrated in previous sections. Increase of average from 2005 to 2012 for ground-level ozone are noticeable in several parts of the US but especially obvious over high plains, foothills, and also in western Canada (Alberta) where positive trend becomes significant and present over large areas. Part of this increase could be attributed to growing regional socio-economic activities (growing oil and gas industries) but could also be partly explained by increasing intercontinental transport originating from emerging countries (Stohl et al., 2002; Cooper et al., 2005; Cooper et al., 2010), an increase of forest fire activity (National Academy of Science, 2011) or a possible increase of vertical transport due to deep stratospheric intrusions. On the other hand, a decrease of the average from 2005 to 2012 is noted mostly in northern California, intermountain regions of US and southern Canada, Texas, around the Great lakes and in New-Brunswick (Canada) and could be attributed to better municipal, state or province air pollution measures and regulation and to economic slowdown as well (see Sect. 5.2).

5.1.2 $PM_{2.5}$

A similar computation is presented for $PM_{2.5}$ in Fig. 12 a, b and c. Table 5b gives the details in % change for all percentiles and statistical moments for each region in the observation space. It is also interesting to note that $PM_{2.5}$ has significantly decreased in eastern US (particularly near and South of the Great Lakes, Fig. 12c) where most of the industrial US activities usually take place. Changes in the range of -1.0 to $-3.0\,\mu g\,m^{-3}$ per year are experienced for a cumulative total of -7 to $-20\,\mu g\,m^{-3}$ for the 7 yr period for that region according to Fig. 12c. Since it is known that $10\,\mu g\,m^{-3}$ change is associated with about 6 % change of death rate (Pope at al., 2002), this improvement should have significantly impacted positively the health of the inhabitants of these re-

ACPD
13, 13967–14035, 2013

gions. On the other hand, significant increase of $PM_{2.5}$ in the western part of North America is expected to reduce the health of exposed people in those regions. The spatial scale of changes in eastern North America (meso-scale) contrasts with that in the West which seems to be more localized (smaller spatial scale). In the East, the decrease suggests a generalized positive effect of anti-pollution measurements adopted through the years which had in turn a successful impact in reducing domestic emissions as mentioned above. As for ozone, in the western part of North America, positive trends for $PM_{2.5}$ noted locally are more symptomatic of growing local socio-economic and industrial activities. But it could also be linked with increase of fire occurrence at specific locations which generates great amounts of $PM_{2.5}$. According to US National Council study, 200–400 % increases in burned area are expected per degree of warming in western US (National Academy of Sciences, 2011). The impact of anti-pollution measures (negative trends) is obvious in eastern parts of US and Canada and in some parts of southern California, while in other geographical areas other factors seem to overshadow these measures where it even reverts to a positive trend such as in northwestern US, intermountain regions as well as Alberta, Canada.

5.2 Decadal trends and inter-annual fluctuations for ozone and $PM_{2.5}$

We believe that inter-annual fluctuations are influenced by five main driving mechanisms: (1) impact of better regulation and anti-pollution measures (2) meteorological fluctuations, (3) socio-economic changes (e.g. recession) (4) increase of background levels due to intercontinental transport, (5) change of stratospheric-tropospheric exchanges and (6) objective analysis errors (i.e. artifacts). Note that the strict use of mathematical average to study trends and inter-annual fluctuations could be misleading because fluctuations could be dampened through the mathematical averaging process itself. This is especially true in the case where the shape of the distribution is changing with time or when trends are spatially inhomogeneous. Therefore, following Cooper et al. (2010) and Vautard et al. (2006), a general trend analysis is computed here by using the percentiles. High percentiles (e.g. 95th, 98th or 99th) changes are

ACPD
13, 13967–14035, 2013

more likely to indicate local changes whereas low percentiles changes rather indicate global or background changes. However, it could also be caused by lesser night urban lower titration of ozone by NO_x (Vautard et al., 2006). According to Fig. 13a and Table 6, ozone high percentiles are decreasing whereas low percentile as well as the median and the mean are all increasing. This implies that the standard deviation of the distribution is changing with time (becoming smaller). For $PM_{2.5}$ (Fig. 13b), a similar situation occurs except that low percentiles are neither increasing nor decreasing (see also Table 6). As mentioned before, the decrease of high percentile is likely associated with successful anti-pollution measures and regulations which act to lower the peak values through time. We believe that the general downward decadal trend of the 95th, 98th and 99th percentile for both ozone and $PM_{2.5}$ (black dashed line in Fig. 13a, b) are robust and are likely to indicate less exceedances of air quality standards and therefore a cleaner air overall in North America especially in the East. It has been reported elsewhere that summertime extreme ozone events in many US urban areas have indeed decreased (Lefohn et al., 2008) which agrees with the results obtained here. However, background ozone are increasing likely due to intercontinental transport from emerging countries (Stohl et al., 2002; Cooper et al., 2010) or from western North America growing oil and gas industry emissions.

Canada's AQS (Canada's air quality standards replacing the Canada's Wide Standards, see http://www.ec.gc.ca/rnspa-naps/default.asp?lang=En&n=07BC2AC0-1) or US NAAQS (National Ambient Air Quality Standards, see http://www.epa.gov/air/criteria.html) are based on high percentiles (e.g. 98th or 99th). It is then appropriate to focus on causes of their inter-annual fluctuations and not only on long-term trends. To study this, we remove the decadal trend (dash black line in Fig. 13a, b) and correlate the inter-annual fluctuations with some selected predictors such as the mean US temperature and the mean monthly precipitation of each summer (June-July-August) for ozone (N = 11 yr, that is 2002–2012) and $PM_{2.5}$ (N = 9, that is 2004–2012). We also have computed the correlations between those fluctuations with known economical indices such as the Industrial Dow Jones (http://upload.wikimedia.org/wikipedia/commons/a/

ACPD
13, 13967–14035, 2013

a6/Dow_Jones_Industrial_Average.png) and various forms of the gross domestic product growth rate (http://www.tradingeconomics.com/united-states/gdp-growth) in order to check for the influences of economic recession on pollution levels. Table 7 (correlation matrix) reveals that the fluctuations (deviation with the decadal tendency removed) of the 95th and the 98th percentile of ozone (dp95-O_3, dp98-O_3) are highly correlated (Pearson's coefficient of correlation above 0.8) with the mean summer (June-July-August) US temperature (tjjaus) and moderately negatively correlated with the precipitation (pjjaus, $R \sim -0.42$ to -0.46). The correlations are also moderately significant with the following economic indices; the US Gross Domestic Product Growth Rate (USGDPGR) of the current warm season (that is a mean from May to October, gdpmo, $R \sim 0.40$), the USGDPGR of the first part of the current year (that is from January to June, e.g. gdpjj with R in the range 0.45–0.69, see Table 7). Correlations with the previous year economic indices are also introduced here to account for inertia that is a lag between deterioration of the economy and the later reduction of human activities (presumably taken place in the following year). Indeed, the USGDPGR of the previous year (gdpmol) shows some moderate correlation. For $PM_{2.5}$, no significant correlation (N/S) was obtained with temperature (tjjaus) but moderate negative correlation with precipitation (pjjaus) as well as moderate correlation with the following economic indices are present: the USGDPGR of the current (i.e. gdpmo with devp98, $R \sim 0.41$) and the previous warm season (i.e gdpmol with devp95 or devp98) as well as with the Dow Jones average of the current summer (dowjja, R in the range of 0.46–0.57). Some of these correlations are moderately (p value in the range 0.05–0.15) to highly significant (p value < 0.05) and suggest that the lower values found during the period 2008–2009 for ozone and 2008–2010 for $PM_{2.5}$ are, at least in part, a signature of the economic recession which hits North America and particularly US during that period. Note that a higher value for ozone (positive devp98, e.g value of percentile 98th above the dash line in Fig. 13a) in the period 2010–2012 is likely caused by higher temperatures during that period. For example, a strong increase (jump of 1.3 °C) of the mean US summer temperature from 2009 to 2010 was recorded,

ACPD
13, 13967–14035, 2013

http://www.ncdc.noaa.gov/temp-and-precip/time-series/. For $PM_{2.5}$ (Fig. 13b), there is no such recovery in 2010 since $PM_{2.5}$ is less sensitive to temperature. To that respect, $PM_{2.5}$ fluctuations reflect somehow better the economic inter-annual fluctuations (as suggested by the correlation matrix, Table 7). Mean US summer temperature tends to be strongly correlated with percentile fluctuations of ozone (devp98 and devp95) whereas most economic indices mentioned above having some significant correlation with dp98 and dp95 for $PM_{2.5}$. It is then fair to speculate that the depression of the $PM_{2.5}$ high percentile (98th percentile and the 95th percentile) are also somehow linked to the depression of economic indices (2008–2010) followed by a recovery in 2011 in North America[2]. A multiple regression model using a stepwise-like procedure establishes the explained variance of the main predictors to the overall model (Stepwise procedure of SAS, Statistical Analysis Software version 9.3). Table 8 presents the regression equation along with the percentage of the statistical model explained by each predictor. For $PM_{2.5}$, gdpmol (previous year warm season gross domestic product growth) rate explains 37 % of the variance of the 98th percentile fluctuations (devp98-PM_{25}) whereas the precipitation (pjjaus) explains 27.5 % of the total variance of the inter-annual fluctuations. The statistical model itself explains 64.5 % (R^2 = 0.645) of the total variance. For ozone, as expected from Table 7, the temperature explains most of the fluctuations for the 98th percentile (76 %) whereas the current warm season USGDPGR (gdpmo in Table 7) explains 11 % of the fluctuations and the USGDPGR from July to December of the previous year (e.g. gdpjdl) explains the remainder (4 %) for a total of 91 % for the whole model. Note that these links between pollution and economy established here have also been observed elsewhere: Castellanos and Boersma (2012) attributed the acceleration of the downward trend of tropospheric NO_2 column over Europe in 2008–

[2]The Dow Jones index and USGDPGR reveals a sharp drop in 2008–2009 and resumes back only in 2011 in US. During the recession, the energy consumption and vehicle-miles travelled statistics in US both experienced as well a sharp drop. (see http://www.epa.gov/aqtrends).

ACPD
13, 13967–14035, 2013

2009 to distinct changes in anthropogenic activity in Europe linked to sharp downturns in gross domestic product caused by the global economic recession.

6 Discussion

Standard chemical re-analyses which use the same model set-up to generate all the historical analyses tend to require enormous amount of human resources and involve very tedious work (e.g., RETRO-40 or MACC projects). On the other hand, multi-year objective analyses as produced in here, are simply off-line objective analysis re-processed from the archived operational model outputs and are less demanding on resources. For example, the computing cost of integration is significantly lower (e.g. could be done on a Linux machine since model outputs are pre-calculated). However, some of the advantages of re-analysis are retained only if care is taken to eliminate the systematic biases at any time in the analyses as in our study. Otherwise, incorrect trends could be produced due to various changes of model versions, emissions out of date, sets, resolution, etc. if the bias is not eliminated in the objective analysis scheme. The long term analyses presented here are unbiased (or have a rather very small biases) and are available on a 21 km grid prior to 2009 and 15 km after 2009. They are also available in terms of hourly, daily, monthly, seasonally, yearly and multi-year averages. The model domain covers all of North America but since surface observations are only dense over continental US and southern Canada, it is only in these regions that observations can constrain the model and that the confidence in the results is high. A typical map of analysis error using Eq. (8) is presented in Fig. 14a for ozone and Fig. 14b for $PM_{2.5}$. In areas where the density of stations is high (see Fig. 2), the analysis error could be 2–4 times lower than in those locations where the density is low. Note that values above a certain threshold are not plotted on the maps because there is insufficient observational data in these regions. Therefore, there is no skill of the analysis (analysis error is the same as model error) in these regions and the analysis is then considered unreliable since affected by model errors and biases. A useful

ACPD
13, 13967–14035, 2013

application of the analysis error map could be in the assessment of an optimal network density. In regions where the analysis error is high (low) it is necessary (unnecessary) to increase the network density.

Our results show that high percentiles of ozone and $PM_{2.5}$ are following a decreasing trend overall in North America and that the eastern part of the US is presenting the largest decreasing trend. Some locations, however, exhibit an increasing trend for the mean ozone and $PM_{2.5}$ such as the northwestern part of North America (northwest US and Alberta). Overall, the low percentiles are generally increasing for ozone whereas there is not trend for $PM_{2.5}$. These ozone and $PM_{2.5}$ trends (shown in Fig. 11c, 12c, 13 and Table 6a, b) are only valid for North America in summer months. These trends cannot be extrapolated for other seasons or projected into the future. For example, applying the OA scheme to produce cold season multi-year analyses show that all percentiles (high and low) for ground-level ozone are increasing during that season (Robichaud, 2011). This result differs from the warm season behaviour presented here but agrees with Cooper et al., 2010. According to these authors, Asian ozone precursor emissions would cause springtime surface ozone to significantly increase in western North America despite the fact that domestic emissions are decreasing. On the other hand, as global temperatures continue to rise, more favorable conditions for ozone formation are likely to occur due to factors such as increases in biogenic and soil emissions (IPCC, 2007; Zheng et al., 2008) and increases in wildfires (IPCC, 2007; Jaffe et al., 2008; Houghton, 2009; National Academy of Science, 2011) so that high percentiles of ozone and $PM_{2.5}$ exhibiting a downward trend during the warm season could potentially exhibit an increase in the future.

The summer time trends in ozone, found in this study, are consistent with observations made in other studies. For example, a review of reported ozone trends by Chan and Vet (2010) found mean positive trends ranging between 0.3–1.0 ppbv yr^{-1}. A study by Vautard et al. (2006) for Europe established a positive trend in ozone levels of 0.65 ppbv yr^{-1}. The above results are consistent with Table 6: e.g. 0.47 ppv/year increase for the median (percentile 50th) and 0.3 ppv/year increase for the mean value.

ACPD
13, 13967–14035, 2013

Finally, it is also important to discuss the spatial scale representativeness of OA. Spatial variability is important and pollutant concentration gradients could be high at times bringing the issue of the local representativeness in the objective analysis, especially in urban environments, into question. Brauer et al. (2010) point out that in some Canadian cities significant spatial variation exists, while in others, $PM_{2.5}$ mass is spatially homogeneous. Therefore, within-city spatial variation of ozone and fine particulate matter ($PM_{2.5}$) is case specific. In urban areas, the spatial variation of NO_x is important in determining the surface ozone urban gradient. It is possible for future work to utilize landuse regression models which are highly correlated with NO_x to capture the urban gradient as a means of producing better data fusion of information at higher resolution. NO_x and ultrafine particles (diameter less than 1 micron) are known to be highly correlated but this correlation does not necessarily hold true for larger particles. Difficulties also arise because primary and secondary $PM_{2.5}$ observations are considered together and treated as one species, however, information on the chemical composition of PM is required in order to elucidate the processes governing production, transport and deposition at different scales and chemical composition differs between and within primary and secondary PM (Hobbs, 1993; Jacobson, 2002; Seinfeld and Pandis, 2006). Furthermore, primary $PM_{2.5}$ exhibits spatial variability over small scales while secondary particles tend to be more uniformly distributed (Blanchard et al., 1999; Pinto et al., 2004). These issues will be addressed as future work in the context of OA.

7 Summary and conclusions

The purpose of this article is twofold: (1) to present multi-year analyses of ground-level ozone and $PM_{2.5}$ over North America during the warm season (1 May–31 October) and (2) to analyze their spatio-temporal long term trends and inter-annual fluctuations. The multi-year analyses themselves form a coherent and continuous dataset for the period 2002–2012 for ozone and 2004–2012 for $PM_{2.5}$. The analyses are freely available upon request. As far as we know, no such multi-year analyses have ever been

ACPD
13, 13967–14035, 2013

presented for both ground-level ozone and $PM_{2.5}$ for North America over a decadal period and at such a high spatio-temporal resolution (hourly analyses; 15–21 km). The analyses are based on a methodology that utilizes a modified optimal interpolation scheme adapted for air quality. It has been obtained through an optimal combination of the CMC's Air Quality Regional Deterministic Prediction System (ARDQPS: composed of CHRONOS 2002–2009 and GEM-MACH 2010–2012) for which model outputs are available for every hour and AIRNow surface observations database (2002–2012) supplemented with extra Canadian stations (not part of the AIRNow program added during the GEM-MACH era). A tuning procedure based on the chi-square statistics was developed and applied online to adjust some sensitive parameters of the error statistics set. This procedure was tested successfully and verification with independent data has shown excellent results. The impact of the adaptive scheme is shown to reduce significantly both the bias and random error. An explicit bias correction scheme was used for $PM_{2.5}$ to further reduce the residual biases.

Long term averages are presented as summer climatology maps (June-July-August) for ground-level ozone and $PM_{2.5}$. The objective analyses obtained are also used to compute trends for ozone and $PM_{2.5}$. Low percentiles of ozone exhibit an upward trend (Southern Canada and US together) while high percentiles of ozone show a downward trend overall for North America during the warm season. Some local exceptions to the overall downward trend in high percentile ozone are found in the northwestern part of North America (northwest US and Alberta) but otherwise the results presented in this study are compatible with other studies that have examined long term trends in ozone (see Chan and Vet, 2010; Vautard et al., 2006).

The decreasing trends in the high percentiles of ozone and $PM_{2.5}$ strongly suggest that domestic emissions reduction have been effective; this is especially obvious for the eastern parts of North America (as expected as a result of the concentration of air pollution sources in that region). The reduction in high percentile concentrations of these pollutants implies that human and environmental health risks associated with air pollutant exposure have decreased over the last decade at least in eastern North America.

ACPD
13, 13967–14035, 2013

However, global (background) transport of ozone is increasing and, combined with climate warming, could produce a further increase in ozone (high and low percentiles) in the future. Moreover, oil and gas industries are still developing in western North America which could lead to increases in ozone and $PM_{2.5}$ in the future.

By running an optimal interpolation scheme adapted to air quality for over a decade or so, a high quality integrated estimate of the two main components of smog has been produced. The multi-year analyses presented here are at high spatio-temporal resolution (15 to 21 km; 1 h) and show a relatively high accuracy with an average absolute systematic error less than 0.6 pbbv and 0.7 $\mu g\,m^{-3}$ respectively for ozone and $PM_{2.5}$ and a random error generally less than 9 ppbv for ozone and under 12 $\mu g\,m^{-3}$ for $PM_{2.5}$ during the warm season.

Finally, a study of inter-annual fluctuations of high percentiles for ozone reveals that, after removing the long term decadal trend, a strong correlation is obtained between high ozone percentiles and mean US summer temperature whereas a moderate correlation is obtained between high percentiles and US Gross Domestic Product Growth Rate (USGDPGR) economic index. For $PM_{2.5}$, moderate correlations between high percentiles of $PM_{2.5}$ and precipitation and with the economic indices (USGDPGR and Dow Jones) are observed. Moreover, a multiple linear regression (stepwise-like procedure) confirms that a significant part of the variance of inter-annual fluctuations of high percentiles is explained by the USGDPGR. For ozone, the fluctuations of high percentiles are largely influenced by temperature and to a lesser extent by the USGDPGR. Economic recession can trigger noticeable short term changes in anthropogenic emissions which can reduce pollution. Sharp downturns of USGDPGR were linked to decreases in industrial, construction, transportation and in other human activities in North America during the recession of 2008–2010. Presumably, this has lead to an analogous decrease in the high percentiles for ozone and $PM_{2.5}$ during that period.

Multi-year analyses as presented here are intended mainly for model evaluation, computation of regional pollution trends and for epidemiological studies. Unresolved issues include the treatment of random high pollution events such as forest fires. In the

ACPD
13, 13967–14035, 2013

case of forest fires, monitoring stations in the vicinity or downwind generally record high levels of $PM_{2.5}$ however, since forest fire emissions are not captured by the operational ARDQPS suite, the OA quality control is likely to reject the monitoring data capturing this type of event. Another unresolved issue is the inability of the long term average or climatology to correctly capture fine-scale pollution gradients. These unresolved issues will be addressed in future work.

Acknowledgements. The first author thanks Véronique Bouchet and Jeff Brook from Environment Canada for encouragement in writing this manuscript, Yulia Zaitseva of CMC for producing most of the analyses runs during the GEM-MACH era (2010–2012), for ozone and $PM_{2.5}$, Alexander Kallaur of Air quality Research Division of Environment Canada for support with the CHRONOS model through the years and the team of the Canadian Meteorological Center for technical support with the GEM-MACH model and observation database. Thanks are also given to Janusz Pudykiewicz for revising and commenting the final version of the document. Finally, both authors acknowledge the free use of surface ozone and $PM_{2.5}$ data from US/EPA AIRNow program, CAPMON and NAPS program managed by Environment Canada.

References

ALA: American Lung Association, http://www.lung.org, 2012.

Allen, G. and Sioutas, C.: Evaluation of the TEOM Method for measurement of ambient particulate mass in urban areas, J. Air Waste Manage. Assoc., 47, 6, 682–689, 1997.

Badot, P. M.: Le point sur le dépérissement forestier en Franche-Comté en regard des hypothèses couramment retenues, in: Annales Scientifiques de l'Université de Franche-Comté, Biologie-Écologie, 5, 31–37, 1989.

Berglund, R. L., Lawson, D. R., and McKee, D. J.: Tropospheric ozone and the environment, Papers from an International Conference, Air and Waste Management Association, 19–22 March 1990, Los Angeles California, 1991.

Blanchard, C. L, Carr, E. L, Collins, J. F., Smith, T. B., Lehrman, D. E., and Michaels, H. M.: Spatial representativeness and scales of transport during the 1995 integrated monitoring study in California's San Joaquin Valley, Atmos. Environ., 33, 4775–4786, 1999.

ACPD
13, 13967–14035, 2013

Blond, N., Bel, L., and Vautard, R.: Three-dimensional ozone analyses and their use for short term ozone forecast. J. Geophys. Res., 109, D17303, doi:10.1029/2004JD004515, 2004.
Brasnett, B.: The impact of satellite retrievals in a global sea-surface-temperature analysis, Q. J. Roy. Meteor. Soc., 134, 1745–1760, 2008.
Brauer, M., Hystad, P., and Poplawski, K.: Assessing the spatial representativeness of the $PM_{2.5}$ and O3: Measurements from National Air pollutant surveillance system. Contract for Environment Canada, Internal document of the University of British Columbia, available at: https://circle.ubc.ca/handle/2429/41543, 2011.
Cashel, P., Newhouse, B. S., and Levetin, E.: Correlation of environmental factors with asthma and rhinitis symptoms in Tulsa, OK, Ann. Allerg. Asthma Im., 92, 356–366, 2004.
Cass, R. G.: Deterioration of materials due to ozone exposure: Current problems and future research, in: Tropospheric Ozone and the Environment, edited by: Berglund, R., Lawson, R. R., and McKee, D. J., AWWMA publications, Pittsburg, 311–320, 1991.
Castellanos, P. and Folkert Boersma, F.: Reductions in nitrogen oxides over Europe driven by evironmental policy and economic recession, Nature Scientific Reports, 2, 1–7, doi:10.1038/srep00265, 2012.
Chappelka, A. H. and Flager, R. B.: Future directions in ozone forestry research, in: Tropospheric ozone and the environment, Papers from an International Conference, Air and Waste Management Association, 19–22 March 1990, Los Angeles California, 1991.
Chan, E. and Vet, R. J.: Baseline levels and trends of ground level ozone in Canada and the United States, Atmos. Chem. Phys., 10, 8629–8647, doi:10.5194/acp-10-8629-2010, 2010.
Chang, J. C. and Hanna, S. R.: Air quality model performance evaluation, Meteorol. Atmos. Phys., 87, 167–196, 2004.
Cooper, O. R., Stohl, A., Hubler, G., Hsie, E. Y., Parrish, D. D., Tuck, A. F., Kiladis, G. N., Oltmans, S. J., Johnson, B. J., Shapiro, M., Moody, J. L., and Lefohn, A. S.: Direct transport of mid-latitude stratospheric ozone into the lower troposphere and marine boundary layer of the tropical Pacific Ocean. J. Geophys. Res., 110, D23310, doi:10.1029/2005JD005783, 2005.
Cooper, O. R., Parrish, D. D., Stohl, A., Trainer, M., Nédélec, P., Thouret, V., Cammas, J. P., Oltmans, S. J., Johnson, B. J., Tarasick, D., Leblanc, T., McDermid, I. S., Jaffe, D., Gao, R., Stith, J., Ryerson, T., Aikin, K., Campos, T., Weinheimer, A., and Avery, M. A.: Increasing springtime ozone mixing ratios in the free troposphere over western North America, Nat. Lett., 463, 20108, doi:10.1038/nature08708, 2010.

ACPD
13, 13967–14035, 2013

Daley, R.: Atmospheric data analysis, Cambridge University Press, New York, USA, 1991.
Daley, R.: The lagged innovation covariance: a performance diagnostic for atmospheric data assimilation, Mon. Weather Rev., 120, 178–196, 1992.
Dee, D. P. and da Silva, A. M.: Data assimilation in the presence of forecast bias, Q. J. Roy. Meteor. Soc., 124, 269–295, 1998.
Fleming, J., van Looan, M., and Stern, R.: Data assimilation for CTM based on optimum interpolation and Kalman filter, paper presented at 26th NATO/CCMS International Technical Meeting on Air Pollution Modeling and its application, NATO Comm. On the challenges of the Mod. Soc., Istanbul, Turkey, 2003.
Fortuin, J. P. F. and Kelder, H.: An ozone climatology base on ozonesonde and satellite measurements, J. Geophys. Res., 103, 31709–31734, 1998.
Gandin, L.: Objective analysis of meteorological fields (Gridrometeorol Izdat, Lenningrad (translation published by the Israel Program for Scientific Translation, Jerusalem, 1965)), 242 pp., 1963.
Gauthier, P., Charrette, C., Fillion, L., Gauthier, P., Charette, C., Fillion, L., Koclas, P., and Laroche, S.: Implementation of a 3-D variational data assimilation system at the Canadian Meteorological Centre, Part I: The global analysis, Atmos. Ocean, 37, 103–156, 1999.
Gervais, P.: Maladie asthmatique et aggression chimique, Rev. Fr. Allergol., 34, 5, 403–407, 1994.
Harris, J. M., Draxler, R. R., and Ottmans, S. J.: Trajectory model sensitivity to differences in input data and vertical transport method, J. Geophys. Res., 110, D14109, doi:10.1029/2004JD005750, 2005.
Hazucha, M. J., Bates, D. V., and Bromberg, P. A.: Mechanism of action of ozone on the human lung. J. Appl. Physiology, 67, 1535–1541, 1989.
Hobbs, P. V.: Aerosol–Cloud–Climate Interactions, Academic Press, 54, 1993.
Hogan, C. M.: Abiotic factor, in: Encyclopedia of Earth, edited by: Monosson, E., and Cleveland, C., National Council for Science and the Environment, Washington DC, available at: http://www.eoearth.org/article/Abiotic_factor?topic=49461, 2010.
Hollingsworth, A. and Lönnberg P.: The statistical structure of short-range forecast errors as determined from radiosonde data, Part I: The wind field, Tellus A, 38, 111–136, 1986.
Horowitz, L. W., Walters, S., Mauzerall, D. L., Emmons, L. K., Rasch, P. J., Granier, C., Tie, X., Lamarque, J. F., Schultz, M. G., Tyndall, G. S., Orlando, J. J., and Brasseur, G. P.: A global

ACPD
13, 13967–14035, 2013

simulation of tropospheric ozone and related tracers: description and evaluation of MOZART, version 2, J. Geophys. Res., 108, 4784, doi:10.1029/2002JD002853, 2003.
Houghton, J.: Global Warming, The Complete Briefing, 4th edn., Cambridge University Press, 2009.
Houtekamer, P. and Mitchell, H.: Data assimilation using an ensemble Kalman filter technique, Mon. Weather Rev., 126, 796–811, 1998.
IPCC, Inter-governmental Panel for Climate Change: The Physical Science Basis, Contribution of Working Group I to the Fourth Assessment Report of the Intergovernmental Panel on Climate Change, Cambridge University Press, 2007.
Jaffe, D., Price, H., Parrish, D., Goldstein, A., and Harris, J.: Increasing background ozone during spring on the west coast of North America, Geophys. Res. Lett., 30, 1613, doi:10.1029/2003GL017024, 2003.
Jacobson, M.: Atmospheric pollution, History, science and regulation, Cambridge University Press, 2002.
Kalnay, E.: Atmospheric Modeling, Data Assimilation and Predictability, Cambridge University Press, 2003.
Kaminski, J. W., Neary, L., Struzewska, J., McConnell, J. C., Lupu, A., Jarosz, J., Toyota, K., Gong, S. L., Côté, J., Liu, X., Chance, K., and Richter, A.: GEM-AQ, an on-line global multiscale chemical weather modelling system: model description and evaluation of gas phase chemistry processes, Atmos. Chem. Phys., 8, 3255–3281, doi:10.5194/acp-8-3255-2008, 2008.
Lefohn, A. S., Shadwick, D., and Oltmans, S. J.: Characterising long-term changes in surface ozone levels in The United States (1980–2005), Atmos. Environ., 42, 8252–8762, 2008.
Liu, G., Tarasick, D. W., Fioletev, D. E., Sirois, C. E., and Rochon, Y. J.: Ozone correlation lengths and measurement uncertainties from analysis of historical ozonesonde data in North America and Europe, J. Geophys. Res., 114, D04112, doi:10.1029/2008JD010576, 2009.
Logan, J. A.: An analysis of ozonesonde data for the troposphere: recommendations for testing 3-D models, and development of a gridded climatology for tropospheric ozone, J. Geophys. Res., 104, 16115–16149, 1999.
Logan, J. A., Megretskaia, I. A., Miller, A. J., Tiao, G. C., Choi, D., Zhang, L., Stolarski, R. S., Labow, G. J., Hollandsworth, S. M., Bodeker, G. E., Claude, H., De Muer, D., Kerr, J. B., Tarasick, D. W., Oltmans, S. J., Johnson, B., Schmidlin, F., Staehelin, J., Viatte, P., and

ACPD
13, 13967–14035, 2013

Uchino, O.: Trends in the vertical distribution of ozone: a comparison of two analyses of ozonesonde data, J. Geophys. Res., 104, 26373–26399, 1999.
McPeters, R. D., Labow, G. J., and Logan, J. A.: Ozone climatological profiles for satellite retrieval algorithms, J. Geophys. Res, 112, D05308, doi:10.1029/2005JD006823, 2007.
Ménard R.: Tracer assimilation, in: Inverse Methods in Global Biogeochemical Cycles Geophysical Monograph 114, AGU, 2000.
Ménard, R.: Bias estimation, in: Data Assimilation, edited by: Lahoz, W., Khattatov, B., and Ménard, R., Springer, 2010.
Ménard, R. and Lang-Ping, C.: Assimilation of stratospheric chemical tracer observations using a Kalman filter, Part II: χ^2– validated results and analysis of variance and correlation dynamics, Mon. Weather Rev., 128, 2672–2686, 2000.
Ménard, R. and Robichaud, A.: The Chemistry–Forecast System at the Meteorological Service of Canada, ECMWF, Global Earth-System Monitoring, 5–9 September, 297–308, 2005.
Ménard, R., Cohn, S., Lang-Ping, C., and Lyster, P. M.: Assimilation of stratospheric chemical tracer observations using a kalman filter, Part I: formulation, Mon. Weather Rev., 128, 2654–2671, 2000.
Mitchell, H., C., Chouinard, C., Charette, C., Hogue, R., and Lambert, S. J.: Impact of a revised analysis algorithm on an operational data assimilation, Mon. Weather Rev., 124, 1243–1255, 1996.
Moran, M. D., Ménard, S., Pavlovic, R., Anselmo, D., Antonopoulos, S., Robichaud, A., Gravel, S., Makar, P. A., Gong, W., Stroud, C., Zhang, J., Zheng, Q., Landry, H., Beaulieu, P. A., Gilbert, S., Chen, J., and Kallaur, A.: Recent Advances in Canada's National Operational Air Quality Forecasting System, 32nd NATO-SPS ITM, 7–11 May, Utrecht, NL, 2012.
National Academy of Science: Climate Stabilization Targets: Emissions, Concentrations, and Impacts over decades to millennia, available at http://www.nap.edu (last access: May 2013), 2011.
Newman-Taylor, A.: Environmental determinants of asthma, Lancet, 345, 296–297, 1995.
Pagowski, M., Grell, G. A., McKeen, S. A., Peckham, S. E., and Devenyi, D.: Three-dimensional variational data assimilation of ozone and fine particulate matter observations: some results using the Weather–Research and Forecasting–Chemistry model and Grid-point Statistical interpolation, Q. J. of Roy. Met. Soc., 136, 653, 2013–2014, 2010.

ACPD
13, 13967–14035, 2013

Paul, J., Fortuin, F., and Kelder, H.: An ozone climatology based on ozonesonde and satellite measurements. J. Geophys. Res., 103, 709–731, doi:10.1029/1998JD200008, 1998.
Pinto, J. P., Lefohn, A. S., and Chadwick, D. S.: Spatial variability of $PM_{2.5}$ in urban areas in the United States, J. of Air Waste Manage. Assoc., 54, 440–449, 2004.
Pope III, C. A., Burnett, R. T., Thun, M. J., Calle, E. E., Krewski, D., Ito, K., and Thurston, G. D.: Lung cancer, cardiopulmonary mortality, and long-term exposure to fine particulate air pollution, J. Am. Med. Assoc., 287, 1132–1141, doi:10.1001/jama.287.9.1132, 2002.
Powell, M. J. D.: An efficient method for finding the minimum of a function of several variables without calculating derivatives, Computer J., 7, 155–162, doi:110.1093/comjnl/7.2.155, 2011.
Pudykiewicz, J., Kallaur, A., and Smolarkiewicz, P. K.: Semi-Lagrangian modeling of tropospheric ozone. Tellus, 49B, 231-248, 1997.
Reeves, F.: Planète Coeur. Santé cardiaque et environnement, Éditions MultiMondes et Éditions CHU Sainte-Justine, 2011.
Reich, P. B.: Quantifying plant response to ozone : a unifying theory, Tree Physiol., 3, 63-91, 1987.
Robichaud, A.: A surface ozone and $PM_{2.5}$ climatology (using an improved optimal interpolation scheme), Presented at the Canadian Society of Chemistry Congress. Montreal, 5–9 June, 2011.
Robichaud, A. and Ménard, R.: Objective analysis of surface ozone and mapping potential environmental impacts in North America in summer, Presented at the Amer. Met. Soc. Congress, Long Beach, California, February 2003.
Robichaud, A., Ménard, R., Chabrillat, S., de Grandpré, J., Rochon, Y. J., Yang, Y., and Charette, C.: Impact of energetic particle precipitation on stratospheric polar constituents: an assessment using monitoring and assimilation of operational MIPAS data, Atmos. Chem. Phys., 10, 1739–1757, doi:10.5194/acp-10-1739-2010, 2010.
Rutherford, I.: Data assimilation by statistical interpolation of forecast error fields, J. Atmos. Sci., 29, 809-815, 1972.
Sandu, A. and Chai, T.: Chemical-data assimilation – an overview, Atmosphere, 2, 426-463, doi:10.3390/atmos203426, 2011.
Schere, K. L., Carmichael, G. R., Grell, G. A., Hoff, R. M., Pierce, R. B., and Derber, J. C.: Summary of workshop on chemical data assimilation and data needs for air quality forecasting,

ACPD
13, 13967–14035, 2013

available at: http://www.oar.noaa.gov/WAQ/workshop05/intro.html (last access: May 2013), 2005.
Seinfeld, J. H. and Pandis, S. N.: Atmospheric Chemestry and Physics: from air pollution to climate change, Wiley-Interscience, 2006.
Skärby, L. and Selldén, G.: The effects of ozone on crops and forests, Ambio, 13, 2, 68–72, 1984.
Stohl, A., Eckhardt, S., Foster, C. C., James, P., and Spichtinger, N.: On the pathways and timescales of intercontinental air pollution transport. J. Geophys. Res., 107, 4684, doi:10.1029/2001Jd001396, 2002.
Stieb, D. M., Burnett, R. T., Smith-Dorion, M., Brion, O., Shin, H. H., and Economou, V.: A new multipollutant, no-threshold air quality health index based on short-term associations observed in daily time-series analyses. J. Air Waste Manage. Assoc., 435–450, doi:10.3155/1047-3289.58.3.435, 2008.
Sun, Q., Wang, A., Jin, X., Natanzon, A., Duquaine, D., Brook, R. D., Aguinaldo, J. G. S., Fayad, Z. A., Fuster, V., Lippmann, M., Chen, L. C., and Rajagopalan, S.: Long-term air pollution exposure and acceleration of atherosclerosis and vascular inflammation in an animal model, J. Am. Medical Assoc., 294, 23, 2005.
Tarasick, D. W., Jin, J. J., Fioletov, V. E., Liu, G., Thompson, A. M., Oltmans, S. J., Liu, J., Sioris, C. E., Liu, X., Cooper, O. R., Dann, T., and Thouret, V.: High-resolution tropospheric ozone fields for INTEX and ARCTAS from IONS ozonesondes, J. Geophys. Res., 115, D20301, doi:10.1029/2009JD012918, 2010.
Tilmes, S.: Verfahren zur Analyse von Messungen atmospharischer Spurengase mit dem Ziel der Assimilation in Chemie–Transportmodellen, Berichte des Deutschen Wetterdienstes, 207, ISBN 3-88148-349-7 (ISSN 0072-4130), Selbstverlag des Deutschen Wetterdienstes, 1999.
Tilmes, S.: Quantitative estimation of surface ozone observations and forecast errors, Phys. Chem. Earth B, 26, 759–762, 2001.
Tingey, D. T., Hosgett, W. E., Lee, E. H., Herstrom, A. A., and Azevedo, S. H.: An evaluation of various alternative ambient ozone standards based on crop yield loss data, in: Tropospheric Ozone and the Environment edited by: Berglund, R., Lawson, R. R., and McKee, D. J., AWWMA publications, Pittsburg, 272–288, 1991.
Tombette, M., Mallet, V., and Sportisse, B.: PM_{10} data assimilation over Europe with the optimal interpolation method, Atmos. Chem. Phys., 9, 57–70, doi:10.5194/acp-9-57-2009, 2009.

ACPD
13, 13967–14035, 2013

van der A, R. J., Allaart, M. A. F., and Eskes, H. J.: Multi sensor reanalysis of total ozone, Atmos. Chem. Phys., 10, 11277–11294, doi:10.5194/acp-10-11277-2010, 2010.
van Donkelaar, A., Martin, R. V., and Park, R. J.: Estimating ground-level $PM_{2.5}$ using aerosol optical depth determined from satellite remote sensing. J. Geophys. Res., 111, D21201, doi:10.1029/2005JD006996, 2006.
van Donkelaar, A., Martin, R. V., Brauer, M., Kahn, R., Levy, R., Verduzco, C., and Villeneuve, P. J.: Global estimates of ambient fine particulate matter concentrations from satellite–based aerosol optical depth: development and application, Environ. Health Persp., 118, 847–855, doi:10.1289/ehp.0901623, 2010.
Vautard, R., Szopa, S., Beekmann, M., Menut, L., Hauglustaine, D. A., Rouil, L., and Roemer, M.: Are decadal anthropogenic emission reductions in Europe consistent with surface ozone observations?, Geophys. Res. Lett., 33, L13810, doi:10.1029/2006GL026080, 2006.
White, M. C., Etzel, R. A., Wilcox, W. D., and Lloyd, C.: Exacerbations of childhood asthma and ozone pollution in atlanta, epidemiology study, Environ. Res., 65, 6–68 doi:10.1006/enrs.1994.1021, 1994.
Wu, L., Mallet, V., Bocquet, M., and Sportisse, B.: A comparison study of data assimilation algorithms for ozone forecast, J. Geophys. Res., 113, D20310, doi:10.1029/2008JD009991, 2008.
Zeng, G., Pyle, J. A., and Young, P. J.: Impact of climate change on tropospheric ozone and its global budgets, Atmos. Chem. Phys., 8, 369–387, doi:10.5194/acp-8-369-2008, 2008.
Ziemke, J. R., Chqandra, S., Labow, G. J., Bhartia, P. K., Froidevaux, L., and Witte, J. C.: A global climatology of tropospheric and stratospheric ozone derived from Aura OMI and MLS measurements, Atmos. Chem. Phys., 11, 9237–9251, doi:10.5194/acp-11-9237-2011, 2011.

ACPD
13, 13967–14035, 2013

Table 1. Summary of environmental and health impacts of ozone and $PM_{2.5}$.

Impact/Surface pollutant	Ozone	$PM_{2.5}$
Oxidizing capacity	– Primary precursor of OH radicals[1]	–
Radiative and climate impact	– Infrared absorber and greenhouse gas[2]	– Through absorption and diffusion of solar light: direct and indirect effect[2].
Environmental impact	– Damage crops and yield loss[3]	– PM can clog stomatal openings of plants and interfere with photosynthesis functions[6]
Health impact	– Increases asthma occurrence, acute and chronic respiratory problems[4]	– Alter lung function, increases cardio-vascular problems and risk of cancer[5]
Damage materials	– Cracking of rubber and polymers[7]	–

[1] Ozone in presence of sunlight decomposes into O_2 and O. The oxygen molecule combines with water vapor to give OH (Jacobson, 2002; IPCC, 2007)
[2] Hobbs (1993); Jacobson (2002); IPCC (2007); Houghton (2009).
[3] Skärby and Sélden (1984); Tingey et al. (1991).
[4] Berglund et al. (1991); White et al. (1994).
[5] Gervais (1994); Pope et al. (2002); Sun et al. (2005); Reeves (2011).
[6] Hogan (2010).
[7] Cass (1991).

ACPD
13, 13967–14035, 2013

Table 2. Number of stations available from US/EPA AIRNow database and Canadian stations for 2005 (CHRONOS era) and 2012 (GEM-MACH era).

	Ozone		$PM_{2.5}$	
	Canada	US	Canada	US
2005	~ 110	~ 1100	~ 100	~ 400
2012	~ 200	~ 1100	~ 190	~ 570

ACPD
13, 13967–14035, 2013

Table 3a. Performance of model and OA for the warm season 2005 (cross validation mode) evaluated using FC2 (frequency of correct value within a factor two when compared to observations) in cross validation mode for ozone for Canada ($N \sim 1440$ observations). Note that Z stands for UTC (Coordinated Universal Time).

CAN ($N \sim 1440$)	FC2 (00Z)	FC2 (06Z)	FC2 (12Z)	FC2 (18Z)
Model	0.700	0.402	0.400	0.805
OA (basic)	0.907	0.662	0.646	0.923
OA adap, no BC	0.914	0.679	0.654	0.927

ACPD
13, 13967–14035, 2013

Table 3b. Performance of model and OA for the warm season 2005 (cross validation mode) evaluated using FC2 (frequency of correct value within a factor two when compared to observations) in cross validation mode for ozone for US ($N \sim 13\,200$ observations). Note that Z stands for UTC (Coordinated Universal Time).

US ($N \sim 13\,200$)	FC2 (00Z)	FC2 (06Z)	FC2 (12Z)	FC2 (18Z)
Model	0.741	0.395	0.340	0.826
OA (basic)	0.904	0.663	0.624	0.965
OA adap, no BC	0.914	0.729	0.641	0.969

ACPD
13, 13967–14035, 2013

Table 4a. As Table 3 but for $PM_{2.5}$ and for the warm season 2007 ($N \sim 1200$ for Canada).

CAN ($N \sim 1200$)	FC2 (00Z)	FC2 (06Z)	FC2 (12Z)	FC2 (18Z)
Model	0.436	0.470	0.420	0.390
OA (basic)	0.453	0.507	0.474	0.435
OA adap, no BC	0.481	0.521	0.530	0.479
OA adap, with BC	0.512	0.521	0.492	0.511

ACPD
13, 13967–14035, 2013

Table 4b. As Table 3 but for $PM_{2.5}$ and for the warm season 2007 ($N \sim 8000$ for US).

US ($N \sim 8000$)	FC2 (00Z)	FC2 (06Z)	FC2 (12Z)	FC2 (18Z)
Model	0.476	0.549	0.523	0.5098
OA (basic)	0.513	0.564	0.581	0.588
OA adap, no BC	0.581	0.586	0.602	0.638
OA adap, with BC	0.670	0.581	0.578	0.699

ACPD
13, 13967–14035, 2013

Table 5a. Percentage changes of OA (2012 minus 2005) for ozone in North America. Positive (negative) values indicate an increase (decrease) from 2005 to 2012.

Ozone (%) change	North America	Eastern Canada	Western Canada	Eastern USA	Western USA
Avg	5.41	6.17	15.48	2.84	7.98
Std dev	−6.22	−9.08	−13.38	−4.86	−5.62
PCT 99	−1.67	−3.70	0.19	−1.12	6.61
PCT 95	−2.07	−2.295	−2.17	−2.91	0.00
PCT 75	1.46	1.43	4.96	−0.92	4.81
PCT 50	7.19	9.52	21.11	4.79	9.65

ACPD
13, 13967–14035, 2013

Table 5b. Percentage changes of OA (2012 minus 2005) for $PM_{2.5}$ in North America. Positive (negative) values indicate an increase (decrease) from 2005 to 2012.

$PM_{2.5}$ (%) change	North America	Eastern Canada	Western Canada	Eastern USA	Western USA
Avg	−25.22	−6.01	−2.89	−22.46	−20.31
Std dev	−11.49	−34.97	21.61	−13.96	0.14
PCT 99	−14.82	−36.98	9.43	−15.52	−8.38
PCT 95	−20.67	−32.76	−0.47	−18.64	−14.65
PCT 75	−22.95	3.64	−1.26	−20.53	−15.50
PCT 50	−27.55	28.57	11.77	−22.89	−26.47

ACPD
13, 13967–14035, 2013

Table 6. Trends for selected percentile (PCT), mean and standard deviation for (a) OA-ozone ($ppbv\,yr^{-1}$) and (b) OA-$PM_{2.5}$ ($\mu g\,m^{-3}\,yr^{-1}$). The p value is given for statistical significance. NS indicates no statistical significance (p value > 0.25). Positive (negative) values indicate an increase (decrease) from 2005 to 2012.

	Trend (O3) ($ppbv\,yr^{-1}$)	p value	Trend ($PM_{2.5}$) ($ug\,m^{-3}\,yr^{1}$)	p value
99th percentile	−0.836	0.076	−1.31	0.022
98th percentile	−0.717	0.060	−1.07	0.016
95th percentile	−0.488	0.071	−0.757	0.014
75th percentile	0.115 (NS)	> 0.25 (NS)	−0.267	0.039
Median	0.470	0.001	−0.0683 (NS)	> 0.25 (NS)
25th percentile	0.71	0.0002	−0.0133 (NS)	> 0.25 (NS)
5th percentile	0.35	0.001	∼ 0 (NS)	> 0.25 (NS)
Mean	0.303	0.0125	−0.177	0.038
Std. dev.	−0.307	0.0045	−0.232	0.054

ACPD
13, 13967–14035, 2013

Table 7. Correlation matrix for fluctuations of high percentile and various predictors. The *p* value indicates the statistical significance of the linear relationship (tjjaus: mean US temperature for June July and August of the current year, pjjaus: mean US precipitation for June July and August of the current year, gdpmo: gross domestic product growth rate from May–Oct of the current year, gdpjj: gross domestic product growth rate of January–June of the current year, gdpmol: same as gdpmo but for the previous year, dowjja: Dow Jones Industrial average for June, July, August of the current year, devp99: deviation of percentile 99 (decadal trend removed), devp95: deviation of percentile 95 (decadal trend removed).

	tjjaus	pjjaus	gdpmo	gdpjj	gpdmo (last y)	dowjja	dp98 O_3	dp95 O_3	dp98 $PM_{2.5}$	dp95 $PM_{2.5}$
tjjaus	1.0	-0.53^{b}	*N/S*	*N/S*	*N/S*	*N/S*	0.82^{a}	0.85^{a}	*N/S*	*N/S*
pjjaus		1.0	*N/S*	*N/S*	*N/S*	*N/S*	-0.42^{c}	-0.46^{b}	-0.43^{c}	-0.44^{c}
gdpmo			1.0	*N/S*	*N/S*	*N/S*	0.41^{c}	0.40^{c}	0.41^{c}	*N/S*
gdpjj				1.0	0.52^{b}	*N/S*	0.56^{b}	0.69^{a}	*N/S*	0.45^{c}
gdpmol					1.0	*N/S*	*N/S*	*N/S*	0.61^{b}	0.57^{c}
dowjja						1.0	*N/S*	*N/S*	0.46^{c}	0.57^{b}
dp98-O3							1.0	0.927^{a}	*N/S*	*N/S*
dp95-O3								1.0	*N/S*	*N/S*
dp98-pm									1.0	0.95^{a}
dp95-pm										1.0

N/S: *p* value > 0.25, [a] *p* value < 0.05, [b] *p* value 0.05–0.15, [c] *p* value 0.15–0.25.

ACPD
13, 13967–14035, 2013

Table 8. Multiple regression models to explain high percentile fluctuations for $PM_{2.5}$ and ozone. The % of the variance explained by each predictor is indicated below each term of the equation.

$PM_{2.5}$ ($N = 9$)			
devp98 = 11.625 + 0.947· gdpmol		−0.1825· pjjaus	
$R^2 = 0.645$	37 %	27.5 %	
($p < 0.1$)			
O_3 ($N = 11$)			
devp98 = −87.7 + 3.776· tjjaus	+0.566· gdpmo	+0.2476· gdpjdl	
$R^2 = 0.91$	76 %	11 %	4 %
($p < 0.15$)			

ACPD
13, 13967–14035, 2013

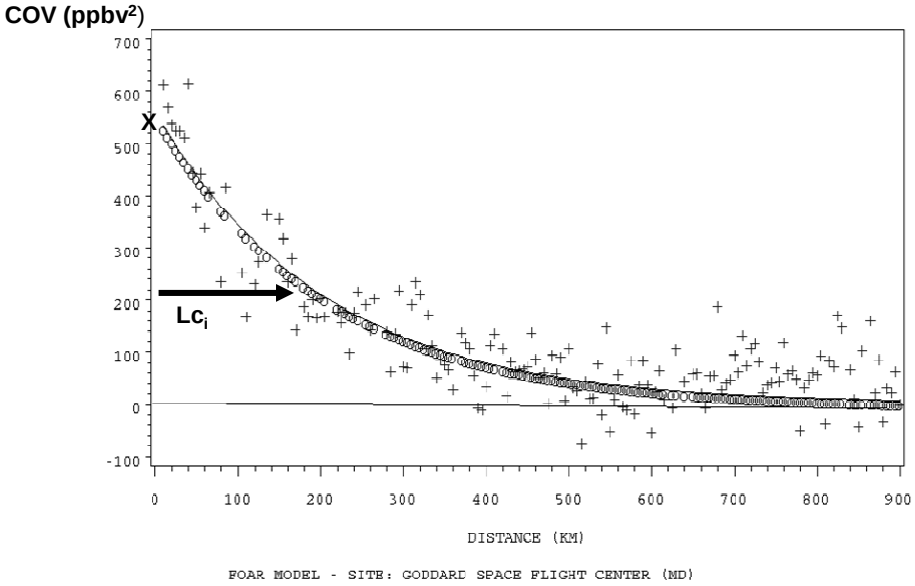

Fig. 1. Determining error statistics from the Hollingsworth and Lönnberg's (H–L) method. Fitting model follows a FOAR (First order autoregressive) model for the error covariance (COV). Note that averages (prior to fit) are calculated in bins of 30 km. The cutoff distance is taken to be 900 kilometers. The intercept of the curve represents the background error variance and Lci, the correlation length (value at 1/e).

ACPD
13, 13967–14035, 2013

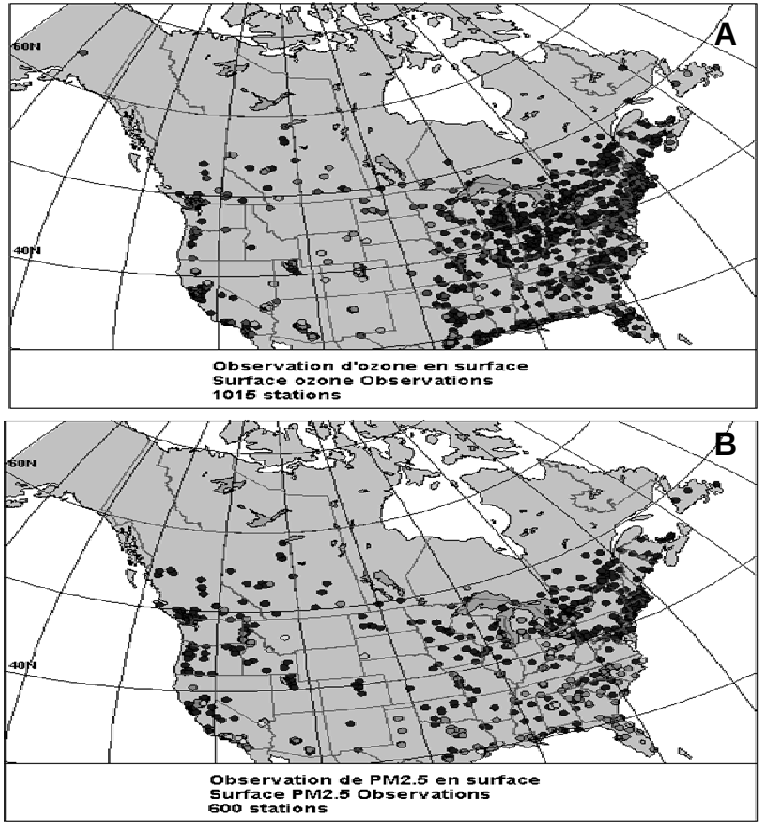

Fig. 2. Map of available observation sites (circa 2010) used for multi-year analyse for **(A)** ozone and **(B)** $PM_{2.5}$.

ACPD
13, 13967–14035, 2013

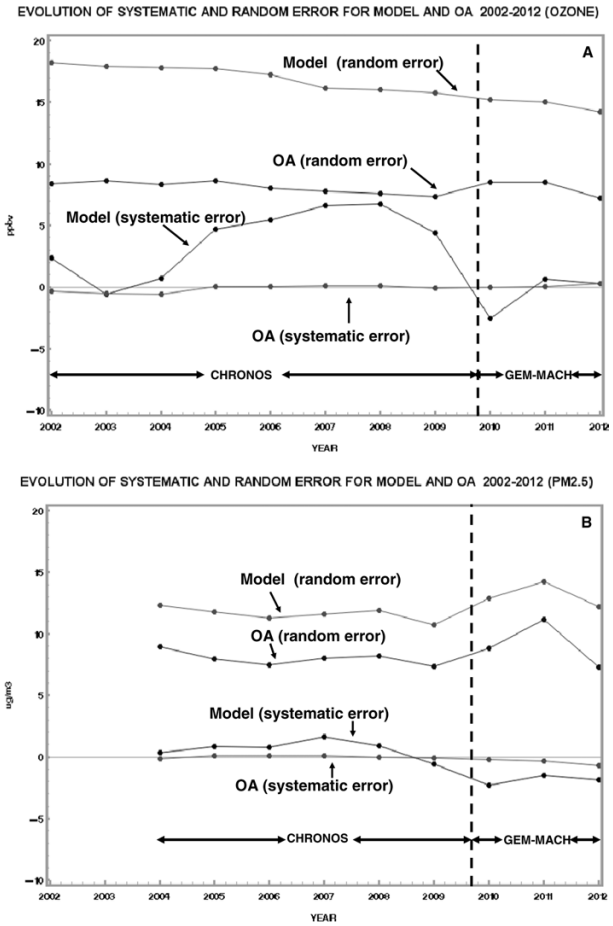

Fig. 3. Evolution of the systematic and random error for model and OA suite for **(A)** ozone (2002–2012), **(B)** $PM_{2.5}$ (2004–2012). The model in use is indicated at the bottom of the figure (e.g. either CHRONOS or GEM-MACH).

ACPD
13, 13967–14035, 2013

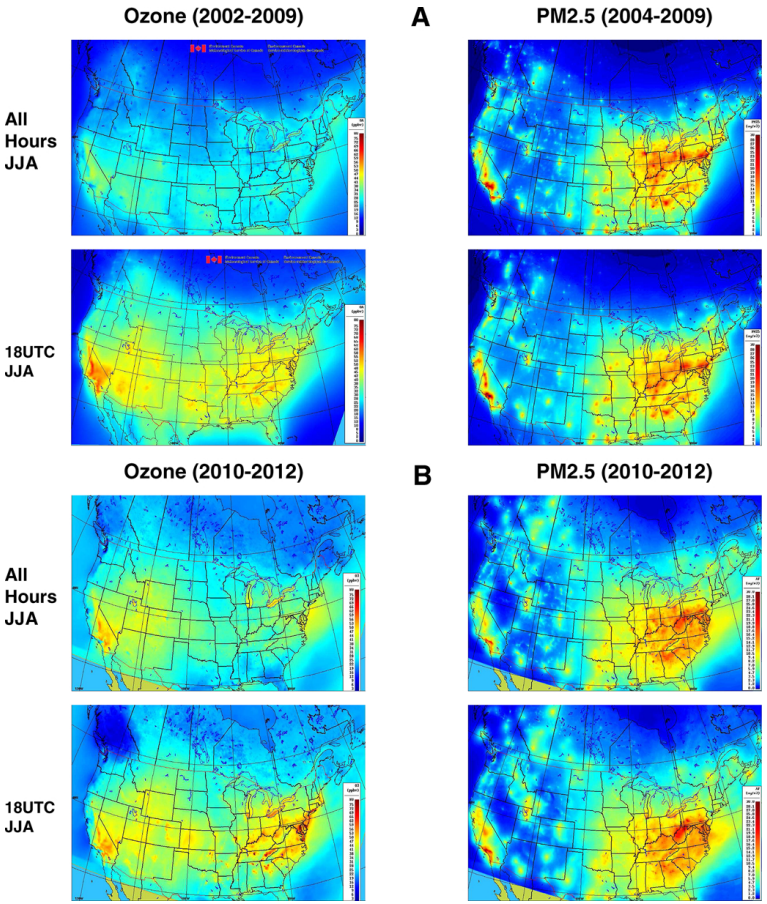

Fig. 4. (A) Long term average OA (CHRONOS era) for summer months June-July-August (JJA) for surface ozone and $PM_{2.5}$. Top left panel: all hours ozone analysis, Bottom left: ozone analysis at 18:00 UTC, Top right: all hours $PM_{2.5}$ analysis, Bottom right: $PM_{2.5}$ analysis at 18:00 UTC. High ozone values are in red and low values are in blue. **(B)** as **(A)** but for the GEM-MACH era.

ACPD
13, 13967–14035, 2013

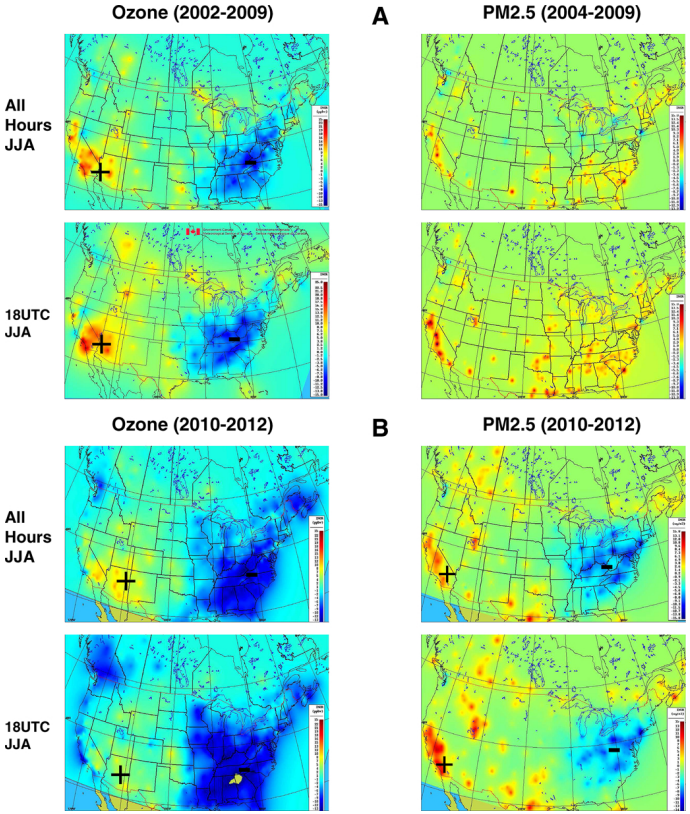

Fig. 5. (A) Long term average analysis increment (CHRONOS era: 2002–2009) for summer months June-July-August (JJA) for surface ozone and $PM_{2.5}$. Top left panel: all hours ozone analysis increments. Bottom left: ozone analysis increments at 18:00 UTC. Top right: all hours $PM_{2.5}$ analysis increments. Bottom right: $PM_{2.5}$ analysis increments at 18:00 UTC. Red values are positive corrections to the model, blue values are negative corrections. **(B)** as **(A)** but for the GEM-MACH era.

ACPD
13, 13967–14035, 2013

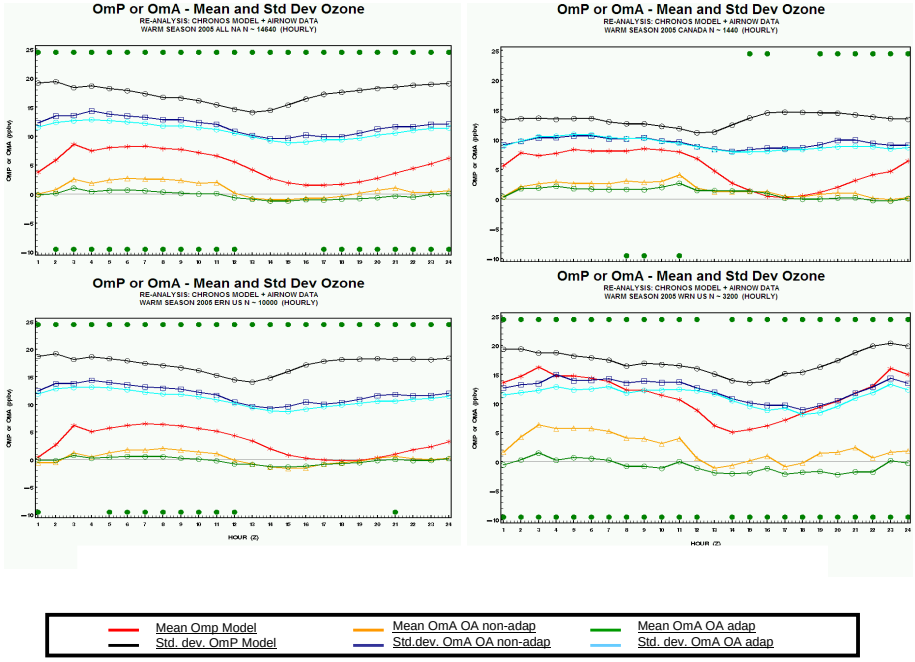

Fig. 6. Warm season cross validation for 2005 (CHRONOS era) for ozone. The diurnal variation of systematic and random errors respectively for model (red and black curves), non-adaptive objective analysis (orange and blue navy) and adaptive OA (green and cyan) are presented for four different regions. Top left panel: all North America, top right Canada, bottom left: Eastern US and bottom right: Western US. Green dots at the top (bottom) of each panel indicate a successful F test variance (T test bias) for statistical significance of the difference between two selected experiments (i.e. adaptive versus non-adaptive scheme).

ACPD
13, 13967–14035, 2013

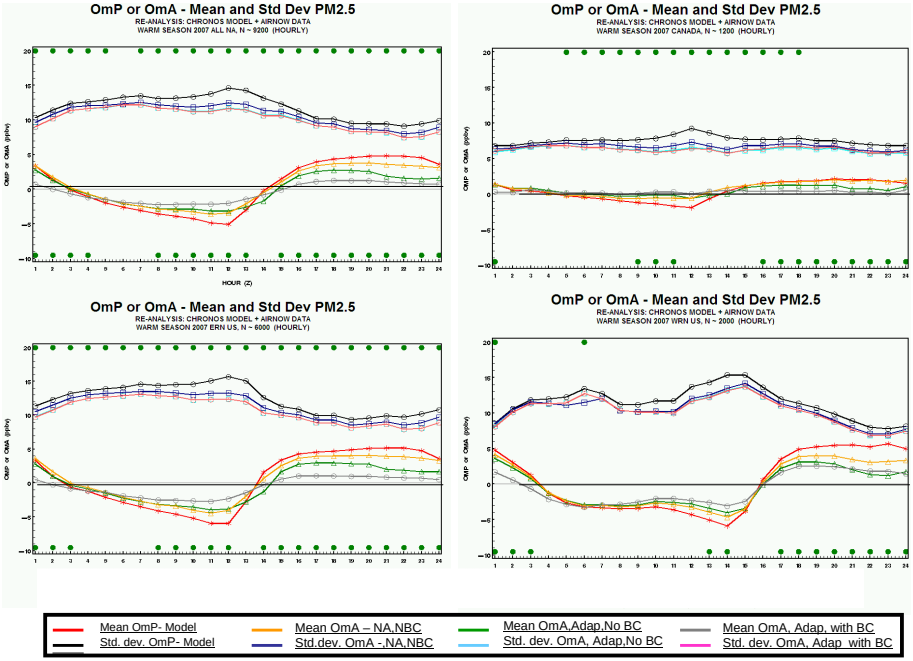

Fig. 7. Cross validation for 2007 for warm season months (CHRONOS era) for $PM_{2.5}$. The diurnal variation of systematic and random errors respectively for model (red and black), non-adaptive Objective analysis (orange and blue navy) and adaptive OA (green and cyan) and adaptive OA with an explicit bias correction (gray and pink) are presented for four different regions. Top left: all North America, Top right: Canada, Bottom left: Eastern US and bottom right: Western US. Significance tests for difference are as in Fig. 6. The differences tested are between the adaptive with bias correction versus the adaptive scheme with no bias correction.

ACPD
13, 13967–14035, 2013

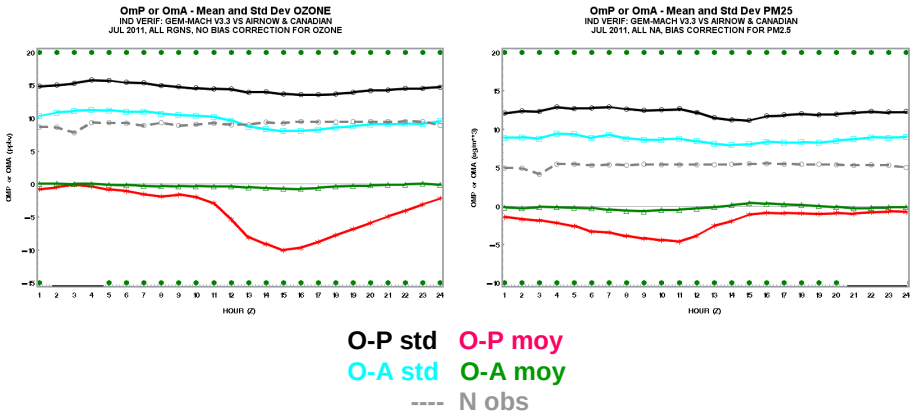

Fig. 8. Cross validation for July 2011 (GEM-MACH era) for ozone (left) and $PM_{2.5}$ (right). Systematic error and random error are respectively shown for OA (green and cyan curve) and for model (red and black curve). Statistical significance tests are as Fig. 6.

ACPD
13, 13967–14035, 2013

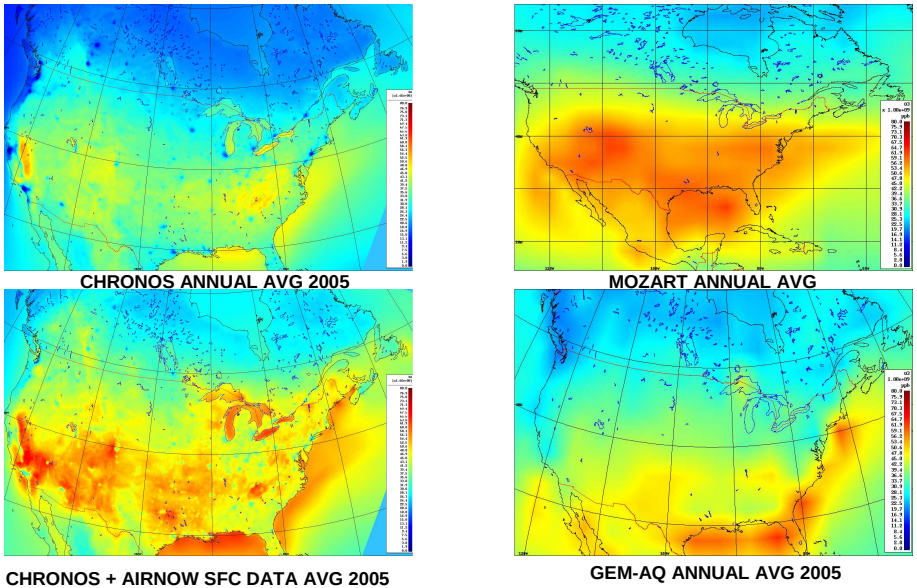

Fig. 9. Comparison of surface ozone OA average for 2005 (all hours, all seasons) with external sources. Top left panel: CHRONOS model 2005 (no observation ingested). Bottom left: OA – average for 2005. Top right: MOZART annual average (version 2). Bottom right: GEM-AQ annual average for 2005. High ozone values are in red, low values are in blue.

ACPD
13, 13967–14035, 2013

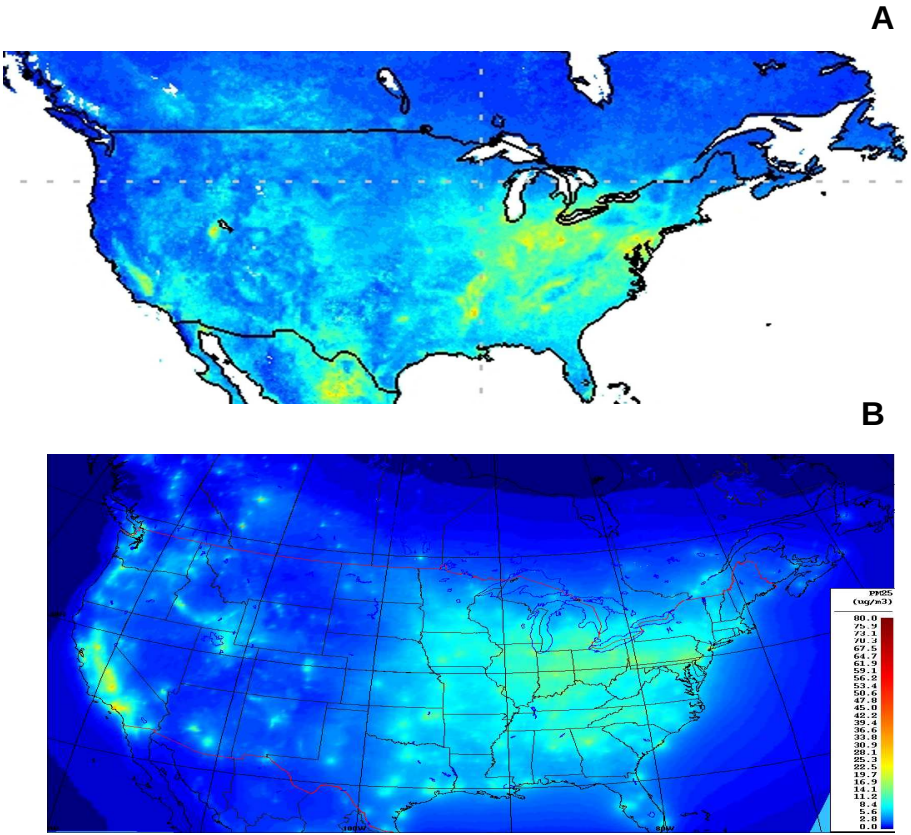

Fig. 10. Comparison of surface $PM_{2.5}$ climatology obtained from **(A)** satellite derived surface $PM_{2.5}$ 2001–2006 (MODIS), van Donkelaar et al. (2010), **(B)** OA $PM_{2.5}$ average for all hours, all seasons 2004–2009 near 18:00 UTC (at approximately the time of satellite overpass). Note that both figures **(A)** and **(B)** have the same colour bar. High values are in red, low values in blue.

ACPD
13, 13967–14035, 2013

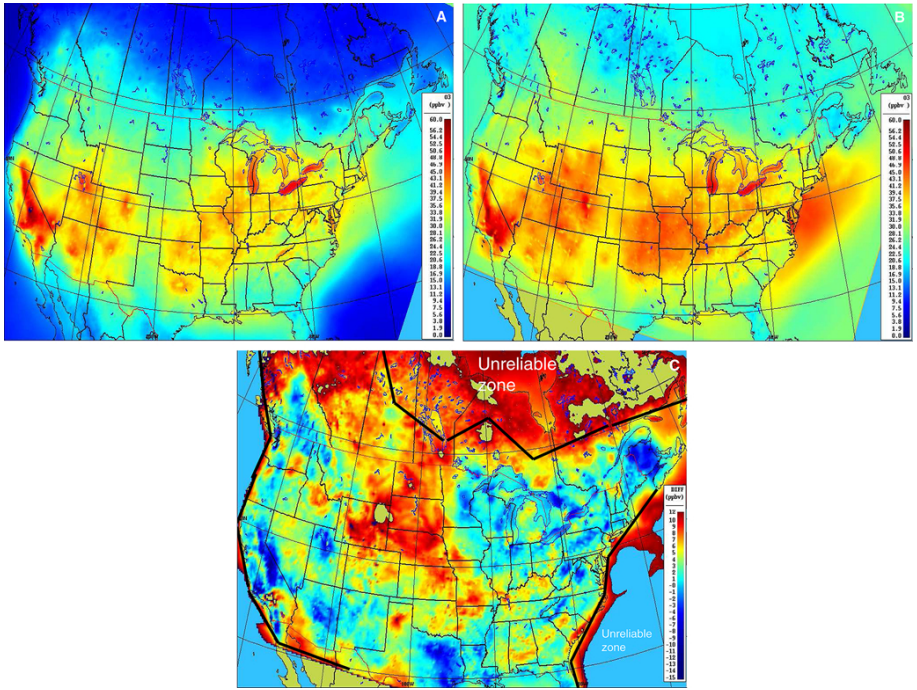

Fig. 11. Comparison of surface average ozone (JJA) in 2012 versus 2005: **(A)** OA ozone 2005 (CHRONOS era), **(B)** OA ozone 2012 (GEM-MACH era), **(C)** difference (OA-2012 minus OA-2005). Note that the area indicated with no OBS are unreliable and caused by model artefacts difference. These zones are also where the analysis error is too high (see Fig. 14a, b).

ACPD
13, 13967–14035, 2013

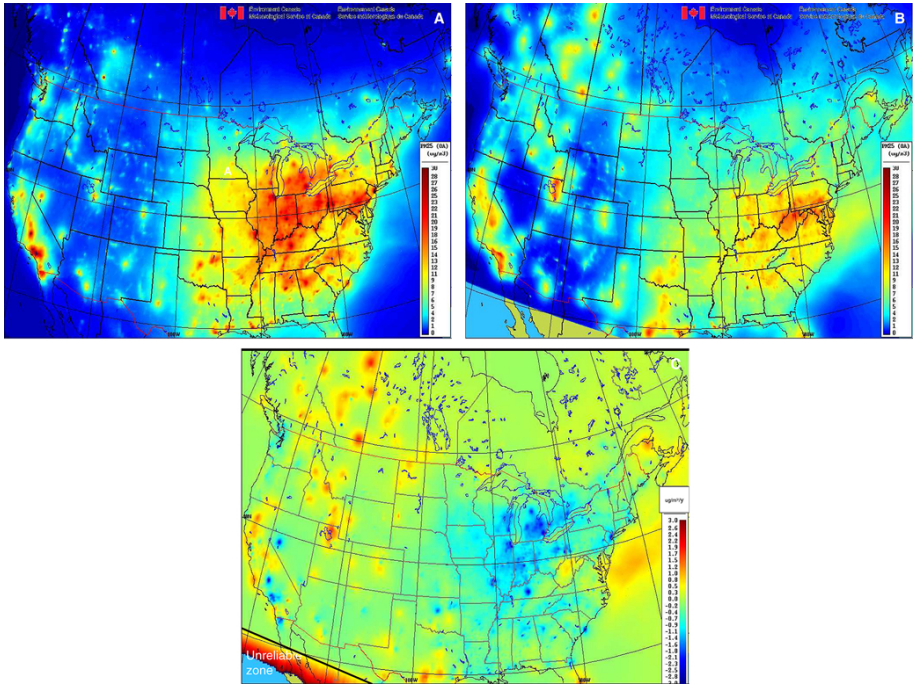

Fig. 12. (A), **(B)** and **(C)** are the same as Fig. 11 but for $PM_{2.5}$.

ACPD
13, 13967–14035, 2013

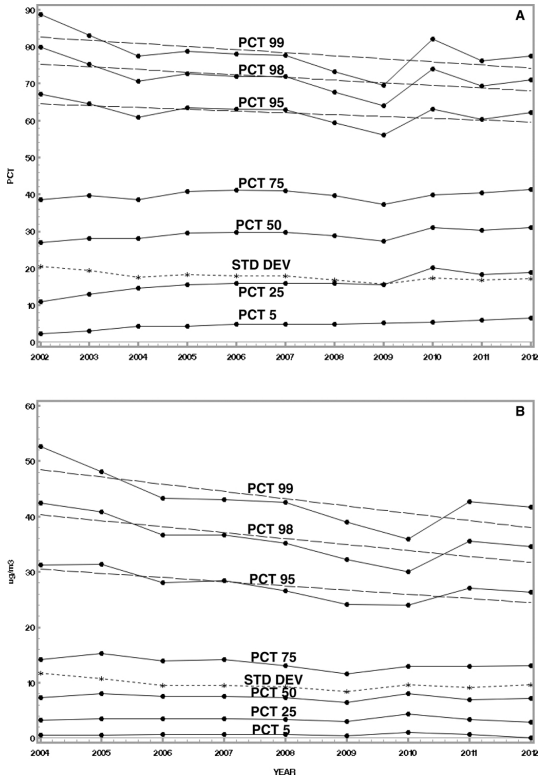

Fig. 13. Long term trend of percentiles (5th, 25th, 50th, 75th, 95th, 98th and 99th) and standard deviation for **(A)** ozone distribution and **(B)** $PM_{2.5}$ distribution. Computations were done in the observation space.

ACPD
13, 13967–14035, 2013

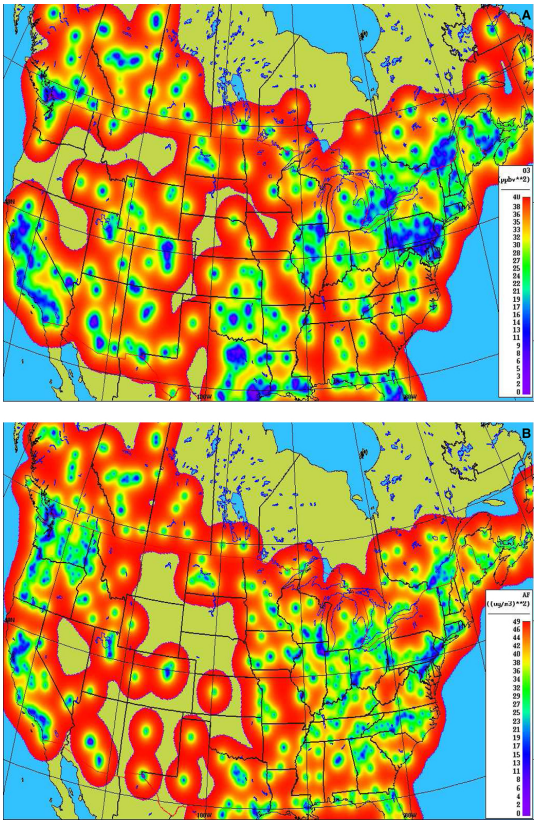

Fig. 14. Analysis errors based on Eq. (8) for **(A)** ozone and **(B)** $PM_{2.5}$. Deep blue corresponds to small analysis errors whereas red to higher errors. The locations where there are no values plotted are where the analysis has no skill (unreliable due to model erratic behavior and/or no observations available to correct model values).

ACPD
13, 13967–14035, 2013